The Plant Cell, Vol. 27: 2616–2636, September 2015, www.plantcell.org

Arabidopsis SEIPIN Proteins Modulate Triacylglycerol Accumulation and Influence Lipid Droplet Proliferation[OPEN]

Yingqi Cai,[a] Joel M. Goodman,[b] Michal Pyc,[c] Robert T. Mullen,[c] John M. Dyer,[d] and Kent D. Chapman[a,1]

[a] Department of Biological Sciences, Center for Plant Lipid Research, University of North Texas, Denton, Texas 76203
[b] Department of Pharmacology, University of Texas Southwestern Medical Center at Dallas, Dallas, Texas 75390
[c] Department of Molecular and Cellular Biology, University of Guelph, Guelph, Ontario, Canada N1G 2W1
[d] U.S. Department of Agriculture-Agricultural Research Service, U.S. Arid-Land Agricultural Research Center, Maricopa, Arizona 85138

ORCID IDs: 0000-0002-0357-5809 (Y.C.); 0000-0001-5483-202X (J.M.G.); 0000-0001-8702-1661 (M.P.); 0000-0002-6915-7407 (R.T.M.); 0000-0001-6215-0053 (J.M.D.); 0000-0003-0489-3072 (K.D.C.)

The lipodystrophy protein SEIPIN is important for lipid droplet (LD) biogenesis in human and yeast cells. In contrast with the single *SEIPIN* genes in humans and yeast, there are three *SEIPIN* homologs in *Arabidopsis thaliana*, designated *SEIPIN1*, *SEIPIN2*, and *SEIPIN3*. Essentially nothing is known about the functions of *SEIPIN* homologs in plants. Here, a yeast (*Saccharomyces cerevisiae*) *SEIPIN* deletion mutant strain and a plant (*Nicotiana benthamiana*) transient expression system were used to test the ability of Arabidopsis SEIPINs to influence LD morphology. In both species, expression of *SEIPIN1* promoted accumulation of large-sized lipid droplets, while expression of *SEIPIN2* and especially *SEIPIN3* promoted small LDs. Arabidopsis SEIPINs increased triacylglycerol levels and altered composition. In tobacco, endoplasmic reticulum (ER)-localized SEIPINs reorganized the normal, reticulated ER structure into discrete ER domains that colocalized with LDs. N-terminal deletions and swapping experiments of SEIPIN1 and 3 revealed that this region of SEIPIN determines LD size. Ectopic overexpression of *SEIPIN1* in Arabidopsis resulted in increased numbers of large LDs in leaves, as well as in seeds, and increased seed oil content by up to 10% over wild-type seeds. By contrast, RNAi suppression of *SEIPIN1* resulted in smaller seeds and, as a consequence, a reduction in the amount of oil per seed compared with the wild type. Overall, our results indicate that Arabidopsis SEIPINs are part of a conserved LD biogenesis machinery in eukaryotes and that in plants these proteins may have evolved specialized roles in the storage of neutral lipids by differentially modulating the number and sizes of lipid droplets.

INTRODUCTION

Lipid droplets (LDs) are subcellular organelles that serve as major reservoirs for carbon storage in eukaryotes and more recently have been associated with other processes, such as stress responses, developmental regulation, membrane trafficking, protein turnover, and lipid signaling (Bartz et al., 2007; Zehmer et al., 2009; Carman, 2012; Herker and Ott, 2012; Murphy, 2012). LDs in plants and other eukaryotes are thought to be derived from the endoplasmic reticulum (ER), whereby newly synthesized triacylglycerols (TAGs) are enriched within the leaflets of the membrane bilayer and form a lens-like structure that subsequently grows in size prior to pinching off to form a mature LD (Jacquier et al., 2011; Chapman and Ohlrogge, 2012; Chapman et al., 2012). While possible mechanisms for LD formation at the ER and several key proteins implicated in this process (e.g., FSP27 [Fat-Specific Protein 27], SEIPIN, FIT2 [Fat Storage-Inducing Transmembrane Protein 2], PERILIPIN1, and FATP1-DGAT2 [Fatty Acid Transport Protein 1-Diacylglycerol Acyltransferase 2] complex) have recently been described in yeast and mammals (Farese and Walther, 2009; Xu et al., 2012; Yang et al., 2012), the general conservation of this ER-LD machinery in plant systems is far less clear.

In plant seeds, LD-associated proteins, such as oleosins, which do not occur outside of the plant kingdom (Huang, 1996), are well characterized and their role in preventing LD fusion during seed desiccation has been documented (Schmidt and Herman, 2008; Baud and Lepiniec, 2010; Rudolph et al., 2011). Oleosins also appear to play an important role in determining LD size during seed development when these organelles are being formed (Miquel et al., 2014). However, beyond oleosins, only a relatively small number of other LD proteins have been identified in plants (Chapman et al., 2013; Gidda et al., 2013; Horn et al., 2013; Szymanski et al., 2014), and their roles in the biogenesis of LDs (including their growth, fusion, turnover, size, and quantity), especially outside of seed tissues, remain mostly unknown. On the other hand, some proteins in mammals and yeast that are involved in LD formation and turnover are conserved in plants (e.g., CGI-58; James et al., 2010; Park et al., 2013), and the heterologous expression of plant oleosins in yeast promotes the formation of LDs from the ER (Jacquier et al., 2013). This suggests that there may be other conserved proteins involved in LD biogenesis in plants and that clues to the compartmentalization of neutral lipids in plant tissues may be gleaned from analysis of LD machinery in other eukaryotes (Chapman et al., 2012).

SEIPIN, mutations in which are responsible for Berardinelli-Seip congenital liposdystrophy in humans, plays an important role in LD biogenesis in humans, mice, *Drosophila melanogaster*, and yeast (Magré et al., 2001; Cui et al., 2011, 2012; Tian et al., 2011;

[1] Address correspondence to chapman@unt.edu.
The author responsible for distribution of materials integral to the findings presented in this article in accordance with the policy described in the Instructions for Authors (www.plantcell.org) is: Kent D. Chapman (chapman@unt.edu).
[OPEN]Articles can be viewed online without a subscription.
www.plantcell.org/cgi/doi/10.1105/tpc.15.00588

Cartwright and Goodman, 2012; Bi et al., 2014). In yeast, SEIPIN is localized to discrete regions of the ER, specifically to ER-LD junctions where nascent LDs are being formed and where the protein functions as an oligomer to somehow influence the assembly of normal-sized LDs containing TAGs and/or sterol esters (Szymanski et al., 2007; Fei et al., 2008; Binns et al., 2010; Wolinski et al., 2011; Yang et al., 2012). Consistent with a role in LD biogenesis, the loss of SEIPIN function in yeast or Drosophila results in abnormal neutral lipid compartmentation, with lipids aggregating at the ER surface (visualized by transmission electron microscopy [TEM]) or accumulating in larger single or aggregates of small LDs within cells (visualized by fluorescence microscopy; Tian et al., 2011; Cartwright and Goodman, 2012). Notably, expression of human *SEIPIN* in either yeast or Drosophila mutants reverses this phenotype, suggesting that *SEIPIN* homologs in different species might have somewhat conserved functions in the biogenesis of LDs (Szymanski et al., 2007; Tian et al., 2011).

In contrast to the single *SEIPIN* gene found in yeast or animals, there are three putative *SEIPIN* homologs in *Arabidopsis thaliana*, *SEIPIN1*, *SEIPIN2*, and *SEIPIN3*, and according to publicly available microarray databases (www.arabidopsis.org), *SEIPIN2* is mostly constitutively expressed in various tissues, while *SEIPIN1* is expressed at highest levels in developing seeds (no expression data are available for *SEIPIN3*; AtGenExpress; Schmid et al., 2005). On the basis of the biological functions of *SEIPIN* homologs in other eukaryotes, we hypothesized that Arabidopsis *SEIPIN*s are involved in LD biogenesis, but the significance of the amplification of *SEIPIN* genes in the plant kingdom is unclear. Here, we tested the functions of Arabidopsis *SEIPIN*s in a yeast (*Saccharomyces cerevisiae*) *SEIPIN* deletion mutant strain and in tobacco (*Nicotiana benthamiana*) leaves, which revealed that each of the three plant SEIPINs has distinct properties in regulating LD number and morphology in both yeast and plants, as well as influencing the reorganization of the ER in plants into what appears to be LD-forming subdomains. Experiments designed to test the regions of Arabidopsis SEIPIN proteins that influenced LD size identified an N-terminal segment that was responsible for modulating LD size. Furthermore, we selected one isoform, SEIPIN1, for overexpression and RNAi suppression studies in Arabidopsis. Analysis of the transgenic plants revealed that increased expression of *SEIPIN1* not only increased the number of larger-sized LDs in Arabidopsis seeds and leaves, but also significantly enhanced TAG accumulation in both tissue types. On the other hand, reduced expression of *SEIPIN1* reduced seed size and the amount of TAG per seed. Taken together, our results reveal that the three Arabidopsis SEIPINs have different, potentially nonoverlapping roles in modulating LD morphology and that when overexpressed increase markedly the accumulation of TAG. Collectively, these findings provide new insights into neutral lipid compartmentalization in plants and may offer novel strategies to manipulate the accumulation and packaging of energy-dense neutral lipids in plant tissues.

RESULTS

Arabidopsis SEIPIN Homologs Share Common Motifs with Human and Yeast SEIPINs

Three putative Arabidopsis SEIPIN homologs (i.e., SEIPIN1, SEIPIN2, and SEIPIN3) were identified by comparing polypeptide sequences of *S. cerevisiae* and human SEIPIN with the Arabidopsis protein database (www.arabidopsis.org). Despite limited overall amino acid sequence similarity (i.e., 34% or less) (refer to Supplemental Figures 1 and 2), at least three common motifs were identified computationally among human SEIPIN, yeast SEIPIN, and the three putative Arabidopsis SEIPINs (Figure 1A; Supplemental Figure 3). Moreover, comparisons of the putative Arabidopsis SEIPIN homologs with each other revealed five motifs that are shared between SEIPIN2 and SEIPIN3, but only three of which are more broadly conserved in SEIPIN1 (Figure 1B; Supplemental Figure 4). Notably, the motifs shared between all three Arabidopsis proteins are localized primarily toward the C-terminal half of SEIPIN2/3, as SEIPIN1 lacks ~150 amino acids in the N-terminal region in comparison to SEIPIN2/3 (Figure 1B; Supplemental Figure 2). Based on these analyses, the putative Arabidopsis SEIPINs appear to share structural features with other eukaryotic SEIPINs, and SEIPIN2 and SEIPIN3 are more similar to each other than to SEIPIN1.

To gain insight into the presence and evolution of the *SEIPIN* gene family in plants, a phylogenetic tree was constructed using sequences derived from representative higher plants, lower plants, and green algae (Figure 1C; Supplemental Data Set 1). This analysis revealed that, similar to yeasts and most mammals, green algae contain just one copy of the *SEIPIN* gene, while the bryophyte *Physcomitrella patens* contains two copies. All higher plants also contain at least two *SEIPIN* genes, one present in a well-defined monophyletic group containing Arabidopsis *SEIPIN1*, and two or more genes present in a second monophyletic group containing Arabidopsis *SEIPIN2/3*. Furthermore, the multiple copies of *SEIPIN* within the latter monophyletic group were generally more similar within a plant species than between plant species. Taken together, these data suggest that there are two distinct types of *SEIPIN* genes in higher plants (i.e., *SEIPIN1* and *SEIPIN2/3*) and that the evolution of these genes in the plant kingdom might correspond to processes associated with land colonization and seed production.

Complementation Analysis of LD Morphology and TAG Accumulation in Yeast *SEIPIN* Deletion Mutants

To test if Arabidopsis SEIPINs have similar functions as yeast SEIPIN in LD biogenesis, the protein coding sequence of each Arabidopsis gene was expressed individually in the *S. cerevisiae* *SEIPIN* deletion mutant strain *ylr404w*Δ, or more recently termed *SEI1* (Szymanski et al., 2007; Fei et al., 2008; Cartwright et al., 2015), then confocal laser scanning fluorescence microscopy was used to assess the sizes and numbers of LDs as a means of testing for functional complementation. As reported previously (Szymanski et al., 2007; Fei et al., 2008), there were fewer, but larger, LDs in the yeast mutant strain compared with either wild-type yeast or the mutant strain transformed with the yeast *SEIPIN* (Sc-*SEIPIN*) gene (Figure 2; refer also to TEM images presented in Supplemental Figure 5). Expression of At-*SEIPIN1* did not reverse either the numbers or sizes of LDs in the yeast mutant strain, but instead increased the average size of LDs dramatically (~4-fold) (Figure 2; Supplemental Figure 5). The sharp delimiting border of the LDs in the At-SEIPIN1-expressing cells reinforced this supersized LD phenotype (compared with the more diffuse appearance of neutral lipid stains often visualized in the *SEIPIN* deletion strain). Expression of At-*SEIPIN2*, and more so

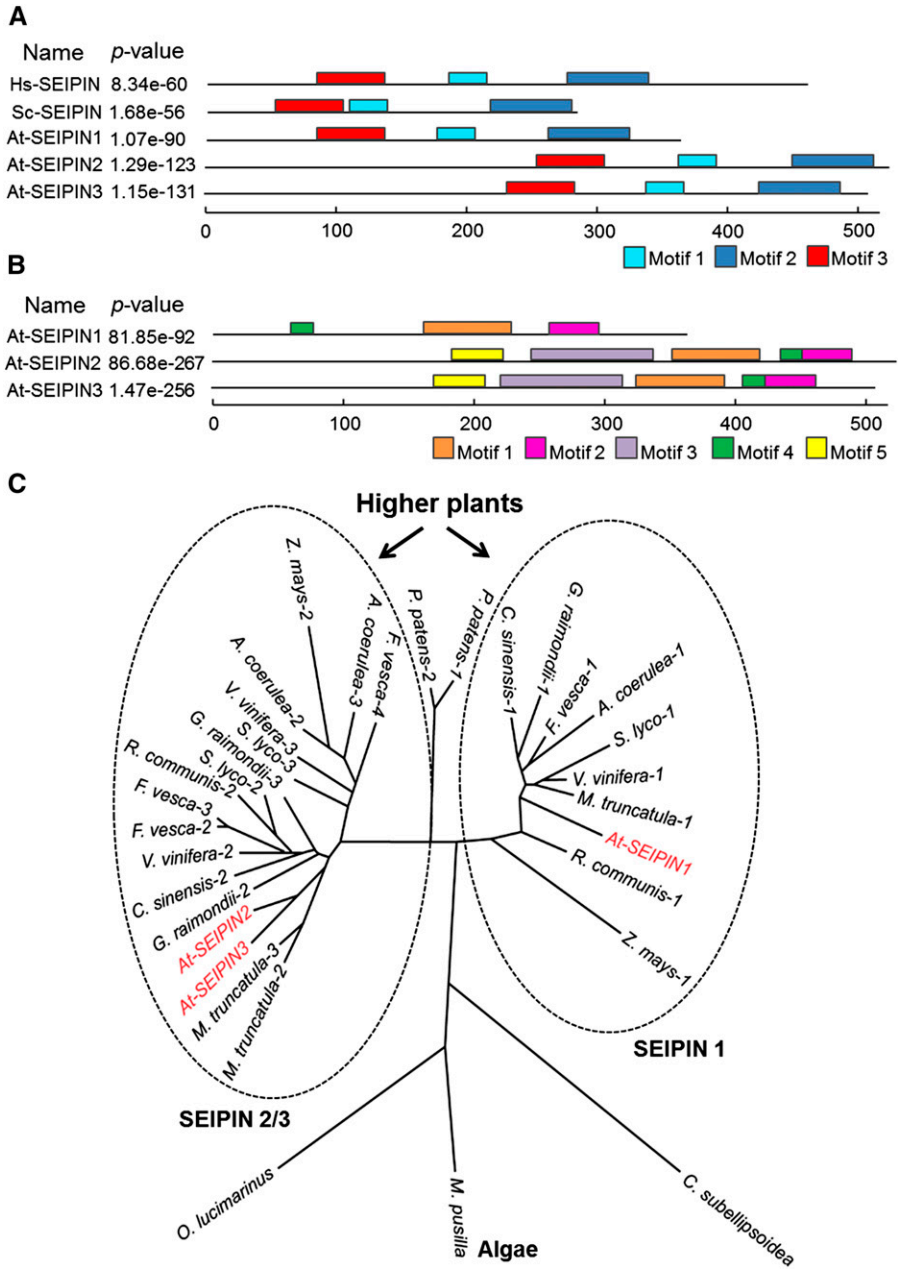

Figure 1. Common Motifs and Phylogenetic Analysis of SEIPIN Proteins in Different Species.

(A) Common motifs shared between SEIPIN homologs in yeast, human, and Arabidopsis. Motif organization was generated by Multiple Em for Motif Elicitation (MEME) (Bailey et al., 2009). The P value gives the probability of a random protein having the same motif. Motifs with P values of <0.0001 are considered to be significant. The minimum width and maximum width of motifs were set at 20 and 300 amino acids, respectively. The minimum number of sites was set at 5.

(B) Common motifs shared between the three Arabidopsis SEIPIN homologs. The minimum width and maximum width of motifs were set as 10 and 300 amino acids, respectively. The minimum number of sites was set at 2.

(C) Phylogenetic analysis of SEIPIN proteins in plants. Homologs of the Arabidopsis SEIPINs were identified in diverse plant species, as well as algae, then phylogenetic analysis was performed as described (see Methods for details). The Arabidopsis SEIPINs are in red font, and the two monophyletic groups are circled.

At-*SEIPIN3*, on the other hand, partially reversed the LD mutant phenotype in yeast by increasing the number of relatively normal size LDs (Figure 2; Supplemental Figure 5). All yeast strains generated more LDs when fed with oleic acid in comparison to the strains fed with glucose, and the LD phenotypes (relative numbers and sizes of LDs) in each strain were even more conspicuous when fed oleic acid versus glucose (refer to Supplemental Figure 6). Taken together, these data reveal that the function of At-SEIPIN2 and At-SEIPIN3 at

least partially overlaps with the SEIPIN protein from yeast, while At-SEIPIN1 generates a novel phenotype, specifically the production of supersized LDs.

Given that TAG is a major component of LDs at the stationary phase of yeast cell growth, we next determined whether the Arabidopsis SEIPIN proteins were able to modulate TAG amount and/or composition in yeast. Total lipids were extracted from the wild type or the deletion strain transformed with each of the Arabidopsis *SEIPIN* genes, and then TAGs were identified and quantified using tandem mass spectrometry. As shown in Figure 3A, the TAG content was reduced slightly in *ylr404w*Δ mutant cells in comparison to the wild type. Expression of yeast *SEIPIN* or any Arabidopsis *SEIPIN*s in *ylr404w*Δ restored the TAGs to wild-type levels, suggesting that Arabidopsis SEIPINs could complement the *SEIPIN* deletion strain in terms of total TAG content (Figure 3A). In the *SEIPIN* deletion mutant, a change in TAG acyl chain composition was observed, which included a significant increase in the proportion of TAG-48:3, TAG-50:3, TAG-52:3, and TAG-54:3 and a reduction in the proportion of TAG-50:1, TAG-52:1, and TAG-54:1 (Figure 3B). Expression of yeast *SEIPIN*, At-*SEIPIN2*, or At-*SEIPIN3* restored wild-type TAG compositions in the *SEIPIN* deletion mutant (Figures 3B and 3C). On the other hand, expression of At-*SEIPIN1* did not reverse the TAG composition of the mutant, but rather enhanced accumulation of the TAG-48:3 and TAG-50:3 molecular species (Figure 3C). Collectively, these results reveal that while all three Arabidopsis SEIPIN proteins functioned similarly to restore TAG levels to wild-type levels in yeast, At-SEIPIN1 functioned differently in comparison to At-SEPIN2/3 in determining composition of the TAG pool. Furthermore, the composition of TAG in cells expressing At-SEIPIN1 was more similar to mutant yeast cells, reinforcing that At-SEIPIN1 is functionally distinct in comparison to these other SEIPIN proteins.

Expression of Arabidopsis SEIPINs in *N. benthamiana* Leaves

To assess the in planta functions of Arabidopsis SEIPINs, SEIPIN1, SEIPIN2, and SEIPIN3 were transiently expressed, individually or in combination, in *N. benthamiana* leaves and the influence on LDs was examined by confocal microscopy (Figure 4A). More specifically, numbers of LDs were counted and grouped in three sizes, either without (i.e., mock or transformation with viral protein P19 only, serving as a suppressor of ectopic gene silencing) or with the SEIPINs (Figure 4B). As shown in Figure 4, all three Arabidopsis SEIPINs elevated the numbers of LDs in leaf cells, but SEIPIN1 produced the relatively largest number of intermediate- and large-sized LDs. By contrast, SEIPIN3 increased significantly the number of small-sized LDs. SEIPIN2 increased the numbers of small- and large-sized LDs significantly but did not generate as many large-sized LDs as SEIPIN1, or small-sized LDs as SEIPIN3, and was therefore intermediate between SEIPIN1 and SEIPIN3. Collectively, these data further support a role for SEIPIN1 in producing larger-sized LDs in eukaryotic cells and further suggest that SEIPIN2 and SEIPIN3 differentially influence the size of LDs in plant cells.

Compared with the expression of SEIPIN1 in leaves by itself, coexpressing SEIPIN2 with SEIPIN1 reduced the number of large-sized LDs by 55% and intermediate-sized LDs by 23%, but generated twice the amount of small-sized LDs (Figure 4). When coexpressing SEIPIN1 and SEIPIN3, the number of large-sized LDs was 36% lower than expressing SEIPIN1 alone and 75% higher compared with expressing SEIPIN3 alone. The number of small-sized LDs in leaves coexpressing SEIPIN1 and SEIPIN3 was lower than in those expressing SEIPIN3 alone, but greater than in those expressing SEIPIN1 alone. The number of intermediate-sized LDs was about the same in leaves expressing SEIPIN1 only and leaves expressing both SEIPIN1 and SEIPIN3. Coexpression of both SEIPIN2 and SEIPIN3 produced similar amounts of large-sized and intermediate-sized LDs as was noted with expression of SEIPIN3 alone. The number of small-sized LDs in leaves coexpressing SEIPIN2 and SEIPIN3 was somewhat between that observed in leaves expressing either SEIPIN2 or SEIPIN3 alone. When all three Arabidopsis SEIPINs were coexpressed, the number of LDs in different size categories was greater than in mock- or P19-transformed leaves. Expression of transgenes in the *N. benthamiana* leaves was verified with RT-PCR (Supplemental Figure 7). Overall, these results suggest that SEIPIN1 facilitates the formation of large-sized LDs preferentially, while SEIPIN2 and especially SEIPIN3 tend to support the formation of small-sized LDs. Expression of combinations of SEIPIN isoforms seemed to combine the features of individual SEIPINS on LD morphology and was not particularly synergistic in LD formation.

The influence of SEIPINs on the formation and morphology of LDs in leaves was also compared with LDs that were induced in leaves by the ectopic expression of the seed-specific transcription factor, Arabidopsis LEAFY COTYLEDON2 (LEC2). LEC2 was shown previously to stimulate the expression of seed-specific proteins and promote oil accumulation in leaves of *N. benthamiana* by shifting the metabolism in leaves to simulate storage lipid biosynthesis in maturing seeds (Santos Mendoza et al., 2005; Andrianov et al., 2010; Petrie et al., 2010). We therefore asked how SEIPINs would function in the tobacco leaf system where TAG synthesis was increased concomitantly via LEC2. As shown in Figure 5, transient expression of LEC2 in *N. benthamiana* leaves significantly increased the number of LDs in all size categories compared with P19-transformed leaves. Furthermore, the number of large-sized LDs was further increased by 83% in leaves expressing both LEC2 and SEIPIN1 relative to those expressing LEC2 alone (Figure 5B), and the increase was similar to the increase when expressing SEIPIN1 alone (Figure 4). Expressing SEIPIN2 or SEIPIN3 increased the number of small-sized LDs by 60 or 200%, respectively, in the LEC2 coexpressing background (Figure 5). Expression of LEC2 and SEIPINs in the *N. benthamiana* leaves was verified by RT-PCR (Supplemental Figure 7). Overall, these data are consistent with a potential role for SEIPINs in modulating the formation and size of LDs in plant tissues, taking particular advantage of the vegetative (leaves) tissue background. Coexpression of SEIPIN isoforms shifted the sizes of LDs in a predictable manner (from studies of SEIPINs alone) in the LEC2 background that was primed for the overproduction of TAG in leaves. However, there did not seem to be an especially large increase in the number of LDs by coexpressing SEIPINs and LEC2 over either alone, but rather SEIPINs influenced the size of LDs in the presence of LEC2.

Neutral Lipid Content and Composition in *N. benthamiana* Leaves Expressing Arabidopsis SEIPINs

Consistent with the confocal microscopy images of LDs described above (Figure 4), the amounts of storage lipids in *N. benthamiana*

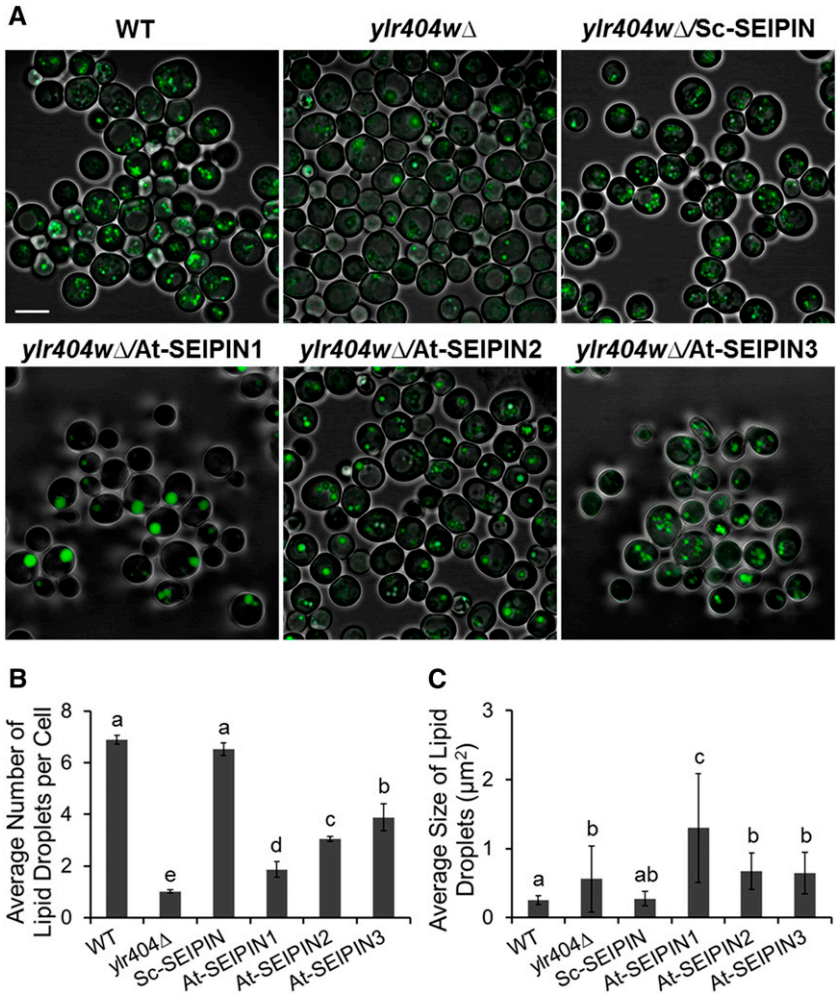

Figure 2. Complementation Tests for LD Phenotypes in the Yeast *SEIPIN* Deletion Mutant (*ylr404w*Δ) by Arabidopsis SEIPINs Compared with Functional Complementation with Yeast SEIPIN (Sc-SEIPIN).

Wild-type (WT) and *ylr404w*Δ were transformed with empty plasmid pRS315.

(A) LD phenotypes were assessed in projections by confocal laser scanning microscopy of different yeast strains. LDs are stained with BODIPY 493/503 and shown in a false color green. Bar = 5 μm.

(B) Numbers of LDs were quantified in different yeast strains (three lines for each strain, with more than 150 cells analyzed per replicate; means with different letters are significantly different determined by one-way ANOVA with Tukey's post-test; $P < 0.05$). SD ($n = 3$).

(C) Average sizes of LD in different yeast strains (30 cells analyzed for each strain; means with different letters are significantly different determined by one-way ANOVA with Tukey's post-test; $P < 0.05$). SD ($n = 30$).

leaves were increased by expressing Arabidopsis SEIPINs (Figure 6). Amounts of storage lipids were estimated two ways: (1) densitometry of TAGs in neutral lipids following thin-layer chromatography (TLC) separations (Figure 6A) and (2) gas chromatography analysis of total fatty acid content in the neutral lipid fraction extracted from leaves (mostly TAGs and sterol esters) (Figure 6B). Of the three Arabidopsis SEIPINs, SEIPIN1 increased TAG content to the greatest extent (87%) relative to mock- and P19-transformed controls, while SEIPIN2 and SEIPIN3 increased TAG content to a lesser degree (56%). TAG content in leaves was further elevated to ~2% of dry weight by coexpressing SEIPIN1 and SEIPIN2, SEIPIN1 and SEIPIN3, or all three Arabidopsis SEIPINs together (Figures 6A and 6B). Coexpression of SEIPIN2 and SEIPIN3 increased the TAG and neutral lipid fatty acids to about the same extent as that in leaves expressing either SEIPIN2 or SEIPIN3 alone. Therefore, it seems that SEIPIN1 has a larger impact on modulating TAG content, perhaps through its ability to facilitate the formation of larger-sized LDs (Figure 4). However, the results in plant cells are somewhat different than in yeast cells, where the increase in TAG was more uniform between the Arabidopsis SEIPINs (compare Figures 3 and 6A). Nonetheless, coexpression of Arabidopsis SEIPINs and LEC2 did not further increase TAG levels significantly (Figures 6A and 6B), suggesting that perhaps LD formation under these conditions is source limited.

Previous studies showed that upregulation of TAG in *Nicotiana tabacum* leaves was accompanied by a change in fatty acid composition of TAG (Andrianov et al., 2010; Winichayakul et al.,

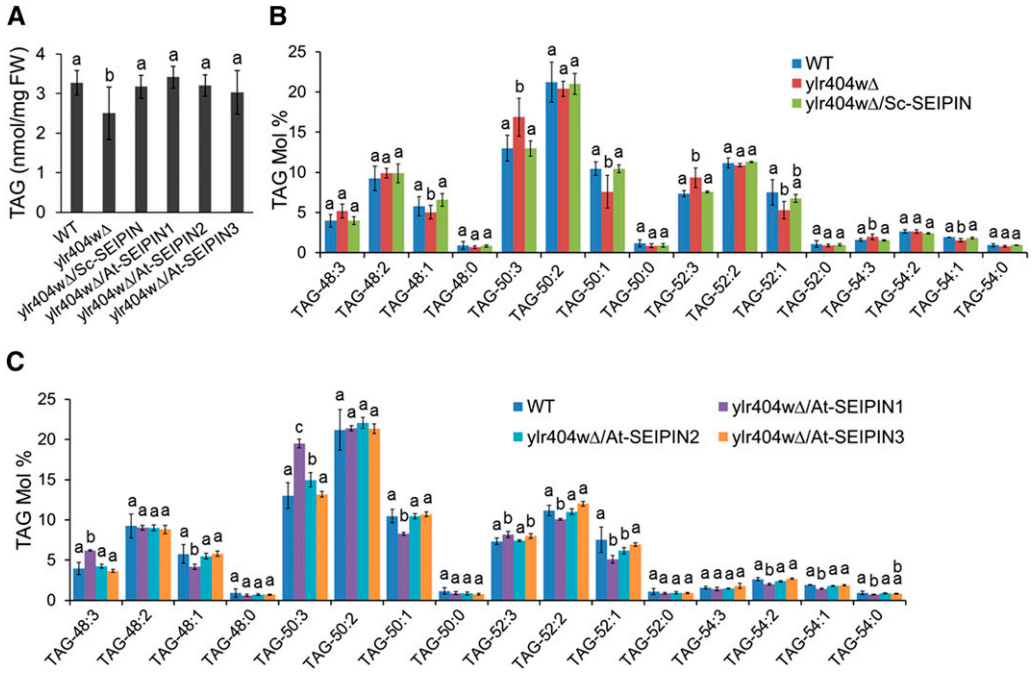

Figure 3. Amount and Composition of TAGs in Yeast *SEIPIN* Deletion Mutant (*ylr404w*Δ) and *ylr404w*Δ Expressing Yeast or Arabidopsis SEIPINs.

Different letters indicate significant difference at $P < 0.05$, as determined by one-way ANOVA with Tukey's post-test. Values are averages, and error bars represent SD ($n = 3$). FW, fresh weight.

(A) Amount of TAG in different yeast strains.

(B) and **(C)** Composition of TAG in different yeast strains.

2013; Vanhercke et al., 2014). Here, the expression of one or more Arabidopsis SEIPINs in tobacco leaves altered the composition of TAGs (Figures 6C to 6E). Leaves expressing SEIPINs alone (Figure 6C) or in various combinations (Figure 6D) generally had more 16:0 acyl moieties and fewer 18:3 acyl moieties in their neutral lipids than mock- or P19-transformed controls (Figures 6C to 6E). Expression of Arabidopsis SEIPINs also reduced the proportion of oleic acid in neutral lipids (Figures 6C to 6E). Similar changes in fatty acid composition that accompanied the increase in leaf TAG also were observed in *LEC2*-expressing leaves (Figure 6E). The differences in fatty acid composition suggest that the pool of acyl groups for TAG are sourced primarily from outside the chloroplast and not likely recycled from plastidial membrane galactolipids, which are richer in 18:3 fatty acids and relatively poorer in 16:0 fatty acids. Hence, this altered composition may be a reflection of the increased source of TAG from ER under these overexpression conditions in leaves as opposed to prevalence of chloroplast acyl lipids as a source of TAG (Chapman and Ohlrogge, 2012; Chapman et al., 2013).

Expression of Arabidopsis SEIPINs Influences the Organization of the ER in *N. benthamiana* Leaves

Because yeast SEIPIN was localized to the ER in yeast cells (Szymanski et al., 2007), we anticipated that Arabidopsis SEIPIN proteins would also localize to, and hence function at, the ER in plant cells. As expected, in *N. benthamiana* leaves transiently expressing the ER marker protein CFP-HDEL (CFP with the KAR2 signal sequence and C-terminal HDEL ER retrieval signal; Szymanski et al., 2007), the ER network appeared to be organized in a web-like reticulate structure that was distributed throughout the cell with a few LDs observed in close proximity to the ER (Figure 7; Supplemental Movie 1). On the other hand, when each of the three Arabidopsis SEIPINs was appended at its N terminus to the GFP and expressed either individually or all together in tobacco leaves, the ER (visualized by coexpressed CFP-HDEL) was dramatically reorganized to form discrete spherical or sometimes tubular-shaped regions that appeared to mostly overlap with both the GFP-tagged SEIPIN(s) and the Nile Red-stained LDs, including the larger- and smaller-sized LDs that were induced in cells expressing GFP-SEIPIN1 and GFP-SEIPIN3, respectively (Figure 7; Supplemental Movies 2 to 5). Similarly, expression of C-terminal GFP-tagged versions of the Arabidopsis SEIPIN1 or SEIPIN3 alone (i.e., in the absence of the CFP-HDEL ER marker protein) in tobacco leaves revealed that both SEIPINs displayed a punctate localization pattern that resembled the reorganized ER described above and that overlapped with most of the LDs in these cells (Supplemental Figure 8), indicating that the position of the GFP moiety appended to the SEIPINs was not responsible for the ER phenotype. We also observed that, at earlier time points after infiltration and expression in tobacco leaves (i.e., 3 d versus 5 d), the GFP-tagged SEIPINs localized to what appeared to be LD-forming sites at the ER, i.e., GFP-SEIPIN1 and GFP-SEIPIN3 localized mostly to specific regions of the CFP-HDEL-labeled ER where LDs were also consistently found. Notably, the ER in these

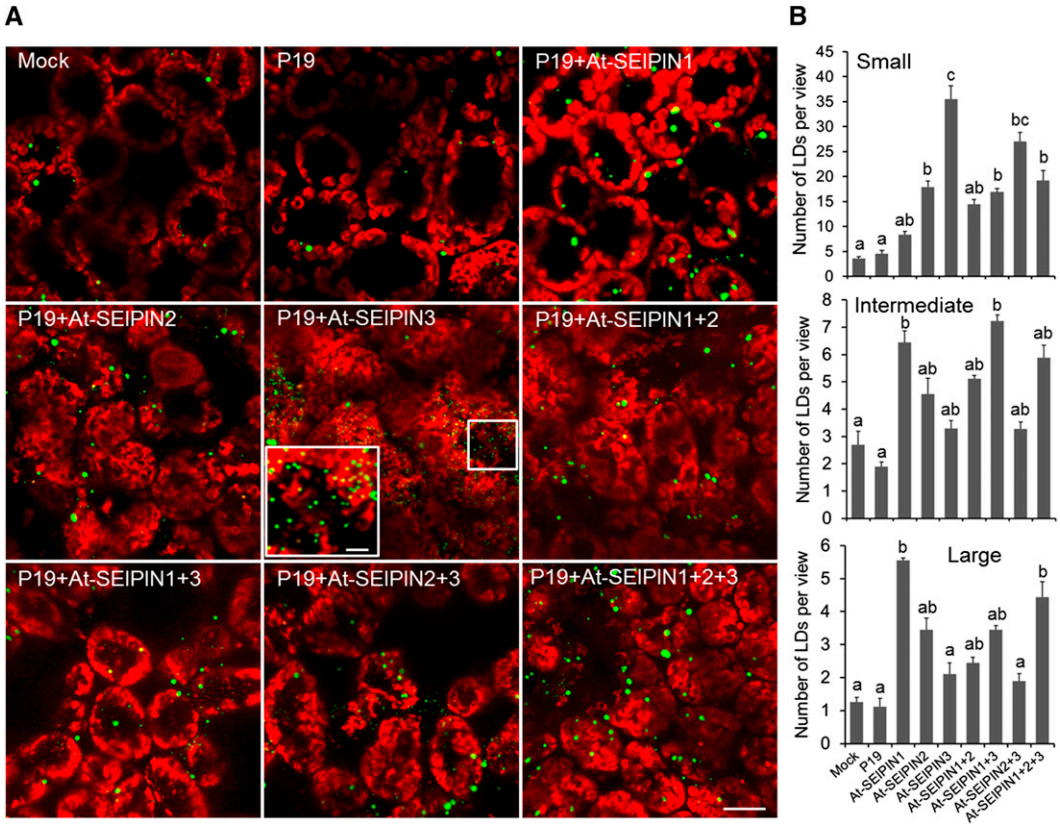

Figure 4. Expression of Arabidopsis SEIPINs in Tobacco Leaves Increases the Number of LDs and Influences Their Size.

(A) Representative confocal images of LDs (BODIPY 493/503 fluorescence, false color green) in tobacco leaves. Red color shows chloroplast autofluorescence. Images were collected at the same magnification and show a 134.82 × 134.82-μm field of the leaf mesophyll. Images are projections of Z-stacks of 22 optical sections taken 0.466 μm apart. Mock infection was infiltrated with media only; P19 was used as a viral suppressor of transgene silencing and was coexpressed in all SEIPIN treatments. Bar = 20 μm; scale bar (zoom in image) = 5 μm.

(B) LD counts by size (average diameter) in tobacco leaves expressing Arabidopsis SEIPINs. Values are averages and SD of three individual experiments (with three images from each replicate). Different letters indicate significant difference at $P < 0.05$, as determined by one-way ANOVA with Tukey's post-test. Small LDs, diameters <1.5 μm; intermediate LDs, diameters between 1.5 and 2.5 μm; large LDs, diameters larger than 2.5 μm.

cells was organized in a more reticulate-like network (Supplemental Figure 9), suggesting that the conspicuous reorganization of the ER at later time points (refer to Figure 7 and Supplemental Figure 9) was a more elaborate exaggeration of LD-forming ER domains that formed over time. Taken together, these results suggest that SEIPINs induce a "reorganization" of the ER into LD-forming domains in plant tissues, and depending on the particular SEIPIN that is expressed, may modulate the size of LDs that are propagated from these domains.

The N Terminus of Arabidopsis SEIPINs Determines LD Size

The striking difference in LD sizes generated by transient expression of the Arabidopsis SEIPINs (Figure 4) prompted us to ask what differences within these proteins might contribute to this phenomenon. Recent studies with yeast SEIPIN indicated that deletion of the N-terminal 14 amino acid sequence immediately upstream of the protein's first putative transmembrane domain (TMD) markedly increased LD size compared with the native, full-length SEIPIN (Cartwright et al., 2015). When aligning the three Arabidopsis SEIPINs (refer to Figure 1B and Supplemental Figure 1), the N terminus was notably shorter in SEIPIN1 compared with SEIPIN3 (and SEIPIN2). Furthermore, protein motifs were shared among the SEIPINs predominantly in the C-terminal two-thirds of the proteins, beginning with the first putative TMD motif (Figure 1B; Supplemental Figure 1), suggesting that the large and small LDs generated by SEIPIN1 and SEIPIN3, respectively, might be influenced by differences in their N-terminal regions. Hence, swaps and deletions of the N-terminal regions up to the first putative TMD of SEIPINs 1 and 3 were designed and their influence on LD size and abundance was evaluated in transient expression assays in tobacco leaves (Figure 8). Results were also compared with the influence of transiently expressed native and N-terminal truncated forms of the yeast SEIPIN protein on LDs in tobacco leaves.

As shown in Figure 8, appending the shorter N-terminal region of SEIPIN1 onto SEIPIN3 (i.e., At-SEPIN1N-3C) resulted in a 9-fold increase in the number of large-sized LDs and an 80% decrease in smaller-sized LDs in tobacco leaves compared with native SEIPIN3.

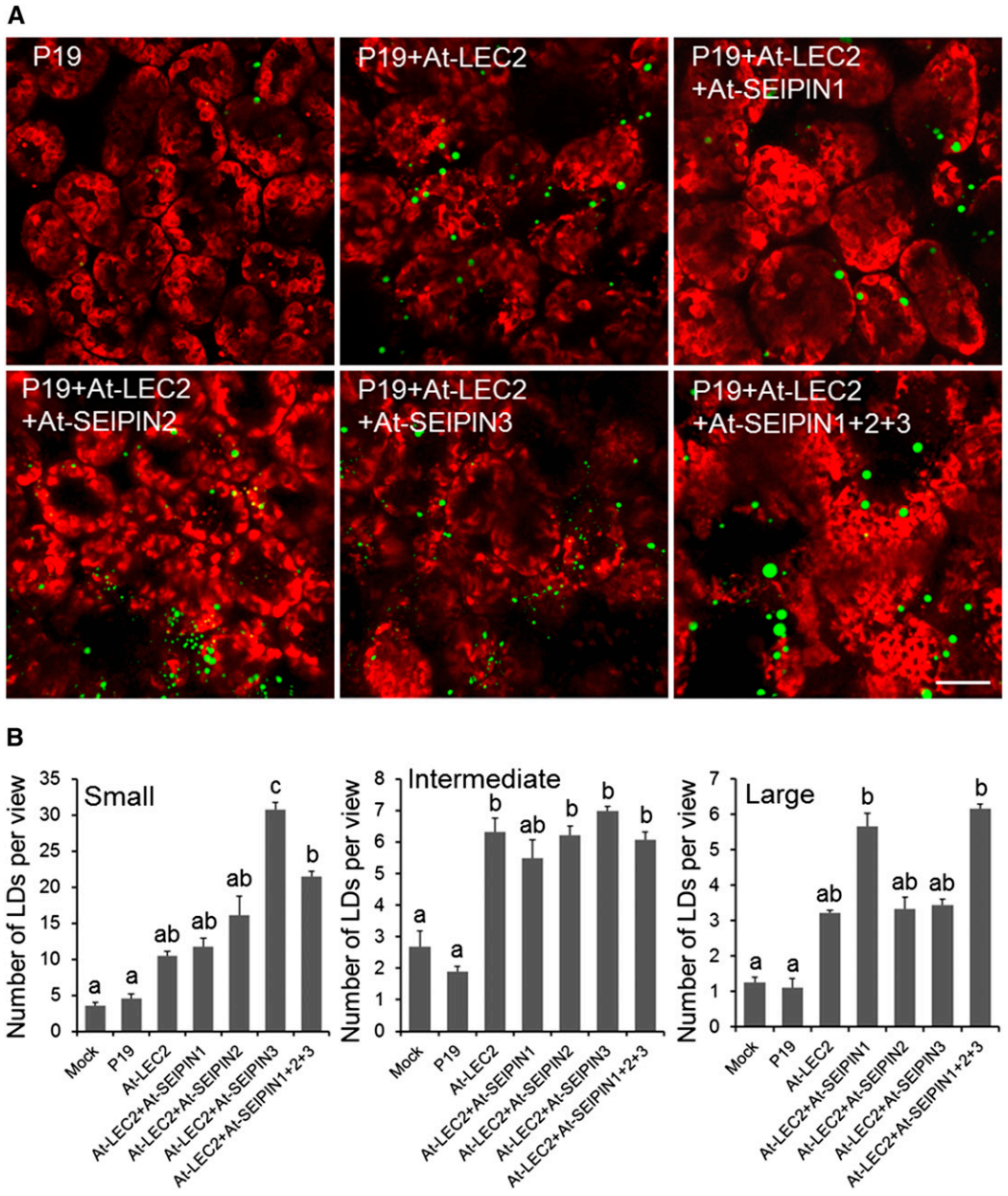

Figure 5. Transient Coexpression of Arabidopsis SEIPINs and LEC2 in Tobacco Leaves.

(A) Representative confocal images of LDs in tobacco leaves. Red color shows chloroplast autofluorescence. Images were collected at same magnification and show a 134.82 × 134.82-μm field of the leaf mesophyll. Images are projections of Z-stacks of 22 optical sections taken 0.466 μm apart. P19 was used as a viral suppressor of transgene silencing in all experiments. Bar = 20 μm.

(B) LD counts by size (average diameter) in tobacco leaves expressing Arabidopsis SEIPINs and LEC2. Values are averages and SD of three individual experiments (with three images from each replicate). Different letters indicate significant difference at $P < 0.05$, as determined by one-way ANOVA with Tukey's post-test. Small LDs, diameters <1.5 μm; intermediate LDs, diameters between 1.5 and 2.5 μm; large LDs, diameters larger than 2.5 μm.

Likewise, truncation of the corresponding N-terminal region in SEIPIN3 (At-SEIPIN3-NΔ) up to the first TMD (red box) also resulted in a 9-fold increase and 80% decrease in large- and small-sized LDs, respectively. By contrast, appending the longer N-terminal region of SEIPIN3 onto SEIPIN1 (At-SEIPIN3N-1C) resulted in a higher number (5-fold) of small-sized LDs. In other words, SEIPIN1 with the N terminus of SEIPIN3 became more like SEIPIN3 in terms of its influence on LD morphology, whereas removal of the longer SEIPIN3 N terminus or swapping the N terminus of the shorter SEIPIN1 onto SEIPIN3 yielded an SEIPIN1-like LD-forming protein.

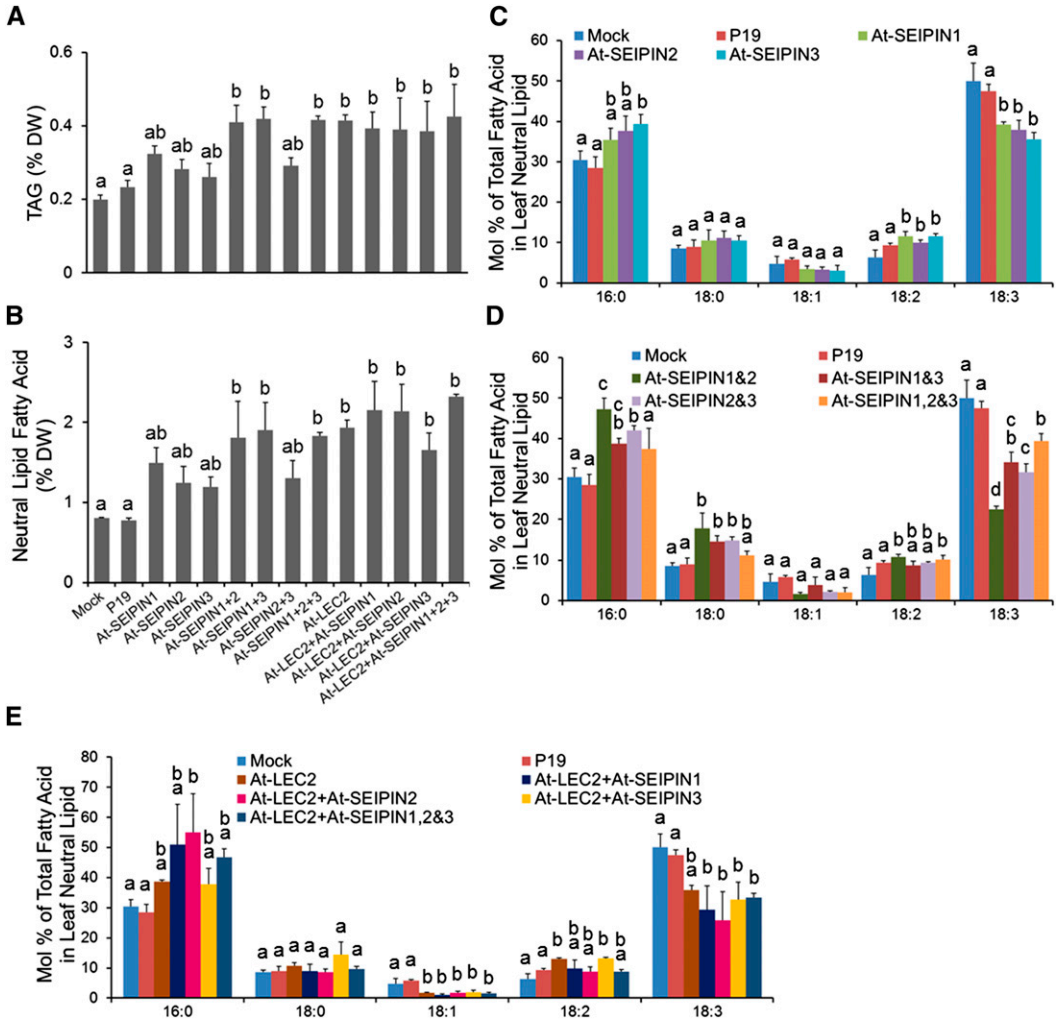

Figure 6. Analysis of TAG and Fatty Acids in Neutral Lipids of Tobacco Leaves Expressing Arabidopsis SEIPINs and/or LEC2.

Values are averages and SD of three individual infiltration experiments. Different letters indicate significant difference at $P < 0.05$, as determined by one-way ANOVA with Tukey's post-test.

(A) Total TAG in tobacco leaves analyzed by TLC and densitometric scanning.

(B) Total amount of neutral lipids on a fatty acid basis in tobacco leaves. DW, dry weight.

(C) to **(E)** Fatty acid compositions in tobacco leaves expressing individual Arabidopsis SEIPINs **(C)**, combinations of Arabidopsis SEIPINs **(D)**, and co-expressing Arabidopsis SEIPINs and LEC2 **(E)**.

Compared with mock- and P19-transformed tobacco leaves, expression of the native, full-length yeast SEIPIN (Sc-SEIPIN) resulted in a modest increase in the number of small-sized LDs, while expression of the N-terminal truncated form of the protein (Sc-SEIPIN-NΔ) yielded significantly more intermediate-sized LDs, although expression of either yeast SEIPIN protein did not produce as many LDs in the plant background compared with the Arabidopsis SEIPIN proteins, especially in terms of large-sized LDs (Figures 8B and 8C). Although it is possible that the yeast SEIPIN was simply not expressed as efficiently in plant cells, it should be pointed out that GFP-tagged yeast SEIPIN proteins were detected in the plant cell background (Supplemental Figure 10). In addition, expression of N-terminal deleted and/or swapped versions of SEIPIN1 and SEIPIN3 appended to GFP at their C termini confirmed that all of the mutant At-SEIPIN proteins examined were expressed and colocalized with LDs in tobacco cells (Supplemental Figure 10), indicating that their intracellular localization was not disrupted by the domain deletions or swaps compared with their native SEIPIN protein counterparts. Furthermore, expression of the yeast SEIPIN resulted in a similar colocalization with LDs in the plant cell background, suggesting a conserved functional role for SEIPINs in LD biogenesis between the eukaryotic SEIPINs.

Expression of Arabidopsis SEIPIN1 in Transgenic Arabidopsis

The large LD phenotype induced by transient expression of SEIPIN1 in yeast and tobacco prompted us to examine the effects of SEIPIN1 in stably transformed plants. As mentioned above,

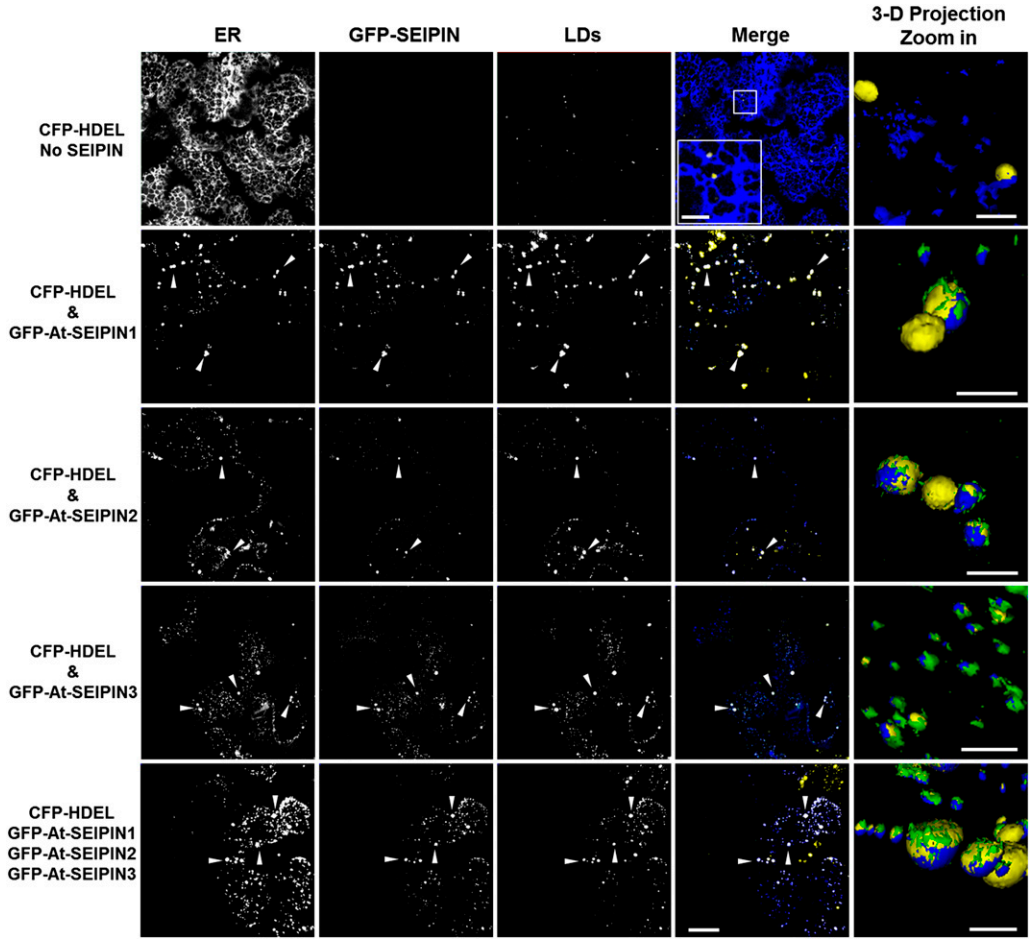

Figure 7. Colocalization of LD, ER, and Arabidopsis SEIPINs in Tobacco Leaves.

Arabidopsis SEIPINs, ER, and LDs were visualized by fluorescence patterns of N-terminal GFP-tagged SEIPINs, CFP-HDEL, and Nile Red, respectively. CFP-HDEL consists of CFP linked to an N-terminal Kar2 signal sequence and C-terminal HDEL ER retrieval signal (Szymanski et al., 2007). All individual channels are shown in gray-scale. GFP, CFP-HDEL, Nile Red, and colocalization are shown in green, blue, yellow, and white, respectively, in the combined channel. Images are all Z-stack projections, and the thickness of stacks varies from 8 to 12 μm to include all CFP signal, GFP signal, and LDs in mesophyll in particular areas. The optical sections were taken 0.466 μm apart. P19 was used as a viral suppressor of transgene silencing in all samples. Arrowheads indicate apparent colocalization of ER, LDs, and GFP-tagged SEIPINs. The images in the last column are 3D projections of surface rendering, high magnified (zoom in) Z-stack images of selected regions of cells showing the colocalization of LDs, ER, and GFP-tagged SEIPINs. Supplemental Movies 1 to 5 are associated with the 3D projections in the last column. Bars in the last column are all 5 μm. Bar (first four columns) = 20 μm. The inset (bar = 5 μm) in the merged image in the top row represents a higher magnification image of a portion of the cell as indicated.

publicly available expression data indicate the SEIPIN1 is expressed mostly in developing seed tissues during the period of rapid oil synthesis (visualized by e-FP browser; Winter et al., 2007), suggesting that SEIPIN1 may have an important role in LD formation in the developing seed embryo. Indeed, RT-PCR confirmed that *SEIPIN1* was expressed mostly in seed (and young seedling) tissues compared with *SEIPIN2* and *SEIPIN3* (Supplemental Figure 11). We asked therefore if constitutive upregulation of SEIPIN1 would influence LD formation in non-seed tissues in Arabidopsis in a manner similar to that in yeast cells and tobacco leaves. Multiple independent Arabidopsis lines with stable, ectopic expression of SEIPIN1, tagged with GFP (SEIPIN1-GFP OE-A, -B, and -C) or untagged (SEIPIN1 OE), resulted in the accumulation of LDs in leaf mesophyll cells (Figure 9), and quantification of these LDs by size (Figures 9B to 9D) confirmed that the increases in LDs were similar to those observed in transiently transformed tobacco leaves (Figure 4). Furthermore, examination of GFP-tagged SEIPIN1 in Arabidopsis leaves revealed that the fusion protein colocalized with many of the LDs, particularly the larger-sized LDs (Supplemental Figures 12A and 12B and Supplemental Movie 6), consistent again with results observed in tobacco leaves. In addition to confirmation of expression through visualization of fluorescent fusion proteins microscopically, RT-PCR confirmed the ectopic expression of GFP-tagged and untagged *SEIPIN1* in transgenic leaves (Supplemental Figure 12C) and also confirmed also the lack of expression of endogenous *SEIPIN1* in nontransgenic (wild-type) leaf tissues.

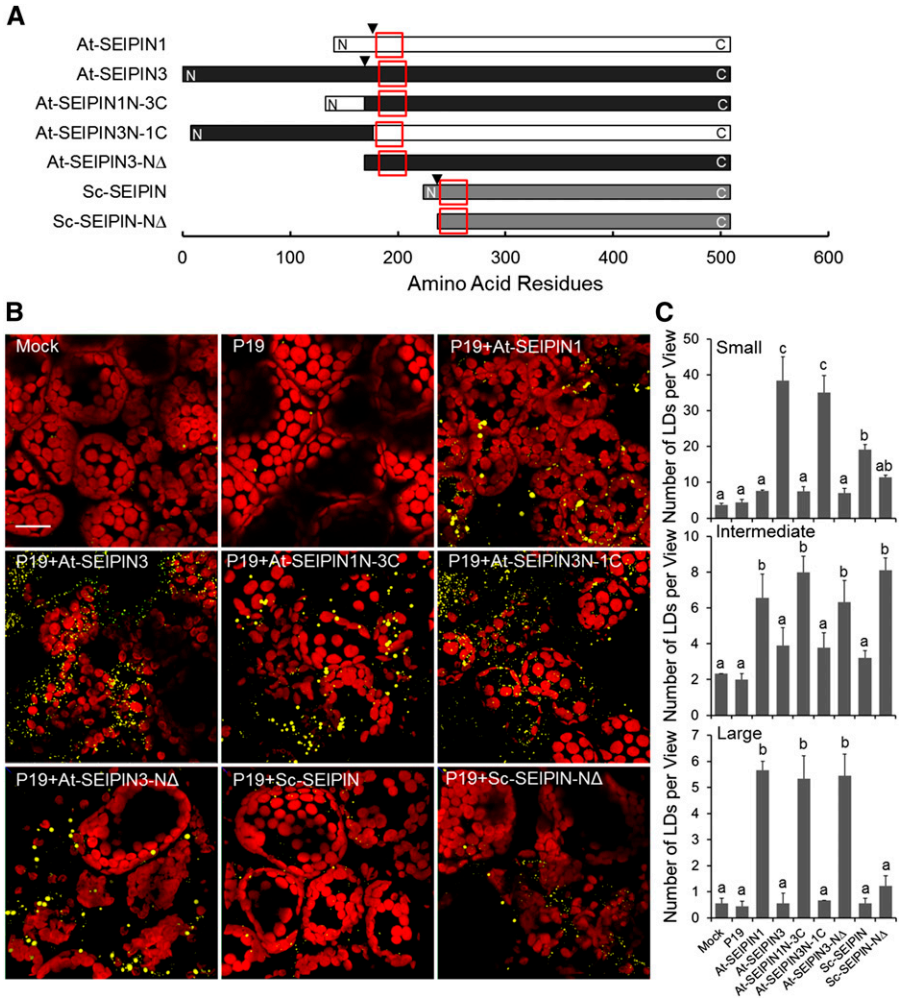

Figure 8. N-Terminal Ends of Arabidopsis SEIPINs Are Involved in Modulating the Size of LDs.

(A) Diagram of N-terminal domain swaps and truncations in At-SEIPIN1, At-SEIPIN3, and Sc-SEIPIN. Black arrowheads indicate the relative position on wild-type At-SEIPIN1, At-SEIPIN3, and Sc-SEIPIN where domain swaps/deletions were introduced. Red box frames indicate the first putative TMD in At-SEIPIN1, At-SEIPIN3, and Sc-SEIPIN.

(B) Representative confocal images of LDs (Nile Red, yellow) in tobacco leaves expressing domain-swapped/truncated Arabidopsis and yeast SEIPINs. Red color shows chloroplast autofluorescence. Images are Z-stack projections collected as described in Figures 4 and 5. Bar = 20 μm.

(C) LD counts by size (average diameter) in tobacco leaves expressing domain-swapped/truncated Arabidopsis and yeast SEIPINs. Values are averages and SD of three individual experiments (with three images from each replicate). Different letters indicate significant difference at $P < 0.05$, as determined by one-way ANOVA with Tukey's post-test. Small LDs, diameters <1.5 μm; intermediate LDs, diameters between 1.5 and 2.5 μm; large LDs, diameters larger than 2.5 μm.

Further examination of Arabidopsis stable homozygous transgenics indicated that overexpression of *SEIPIN1* also facilitated the formation of large-sized LDs in mature seeds (Figure 10) whether these LDs were imaged either in cotyledon cells in situ (Figure 10A) or after being isolated by flotation centrifugation (Figures 10B and 10D). Overall, the marked increase in size of many LDs in Arabidopsis embryos was observed in all of the independent transgenic lines expressing *SEIPIN1* with or without a GFP fusion. This large LD morphology phenotype was also clearly evident in mature seed sections examined by transmission electron microscopy (Supplemental Figure 13), confirming that images obtained via confocal microscopy were indeed large LDs and not clusters of small LDs. Interestingly, the overexpression of *SEIPIN1* in embryos also resulted in an increase in oil content in mature seeds and seed size (Figures 10C, 10E, and 10F), suggesting that the packaging of TAG into LDs may represent a regulatory point that limits storage lipid accumulation in oilseeds.

Although no publicly available T-DNA loss-of-function *SEIPIN1* mutants have been identified in Arabidopsis, we generated knockdown lines by RNAi with reduced *SEIPIN1* expression to examine whether reduced *SEIPIN1* expression influences LD morphology and/or oil accumulation in embryos. In six separate lines derived from three transgenic events, *SEIPIN1* transcripts were reduced markedly, but not eliminated (Figure 11C). While LD

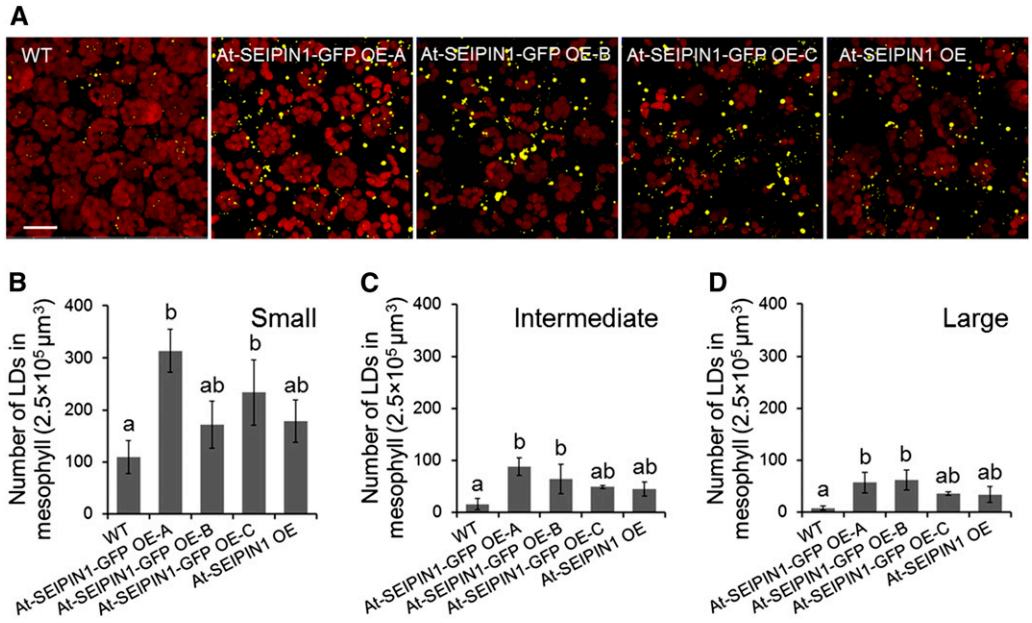

Figure 9. Stable Expression of Arabidopsis SEIPINs Increases the Number and Size of LDs in Arabidopsis Leaves.

(A) Representative confocal images of LDs (Nile Red, yellow) in Arabidopsis leaves. SEIPIN1-GFP OE-A, B, and C are three transgenic events. Red color shows chloroplast autofluorescence. Images were collected at the same magnification and show a 134.82 × 134.82-µm field of the leaf mesophyll. Images are projections of Z-stacks of 30 optical sections taken 0.466 µm apart. Bar = 20 µm.

(B) to **(D)** LD counts by size (average diameter) in Arabidopsis leaves expressing Arabidopsis SEIPINs. Values are averages and SD of three biological replicates (three Z-stack image series from each biological replicate). Different letters indicate significant difference at $P < 0.05$, as determined by one-way ANOVA with Tukey's post-test.

(B) Number of small LDs with diameters <1.5 µm.

(C) Number of intermediate LDs with diameters between 1.5 and 2 µm.

(D) Number of large LDs with diameters larger than 2 µm.

size did not appear to be dramatically altered based on light microscopy (Figure 11A), overall seed size was reduced in all transgenic lines (Figures 11B and 11D). Oil content on a seed weight basis was significantly reduced in one line (i.e., seipin1-7-7), but on a per seed basis, oil content was reduced in all lines (Figures 11E and 11F), suggesting that the reduction in *SEIPIN1* expression contributed specifically to a reduced accumulation of oil per seed and this was manifested as reduced overall seed size. Taking the overexpression and suppression data together, it appears that SEIPIN1 is an important factor for modulating oil accumulation in plants, and it is likely that SEIPIN1, and Arabidopsis SEIPINs in general, enhances the efficiency with which storage lipids are vented from the ER during LD biogenesis. Furthermore, it seems that SEIPIN1 may be specialized to facilitate larger amounts of TAG release from the ER, thus influencing the ultimate size of LDs, which was especially exaggerated when SEIPIN1 was overexpressed. Thus, in seed tissues, where TAG accumulation rates are substantial, alterations in *SEIPIN1* expression exhibited visible, lipid-related phenotypes that impacted overall seed oil yields.

DISCUSSION

SEIPIN homologs in yeast and animal systems are believed to play an important role in lipid storage, especially in regulating the formation of LDs (Szymanski et al., 2007; Fei et al., 2011a). Indeed, genetic mutations in the human *SEIPIN* gene lead to congenital lipodystrophy and inefficient compartmentalization of storage lipids; similarly, the deletion of *SEIPIN* in yeast cells leads to aberrant packaging of neutral lipids (Cartwright and Goodman, 2012). However, there is essentially no information on the occurrence or function of *SEIPIN* homologs in plants, and given the overall paucity of data for LD biogenesis in plant systems, especially outside of seed tissues, the studies described here represent important early steps in understanding the extent of conservation of the subcellular processes involved in compartmentalizing neutral lipids in diverse eukaryotic organisms.

Here, we demonstrate that Arabidopsis has three *SEIPIN* homologs and that they all influence the formation and morphology of LDs in both yeast and plant systems, suggesting that SEIPIN is part of an evolutionarily conserved subcellular machinery for LD biogenesis. On the other hand, these three Arabidopsis *SEIPIN* homologs differed from each other in their ability to function in place of *SEIPIN* in yeast and in their subcellular consequences when expressed in yeast or plant cells. For instance, while all three of the plant SEIPINs were localized to the ER in plant cells (Figure 7), and SEIPIN2 and SEIPIN3 were similar to each other in terms of their ability to partially reverse the LD phenotypes in *SEIPIN*-deficient mutant yeast, SEIPIN1 could not reverse these defects. Generally, SEIPIN1 produced one or two larger-sized ("super-sized") LDs in yeast cells, whereas SEIPIN2 and SEIPIN3 appeared to partially restore the

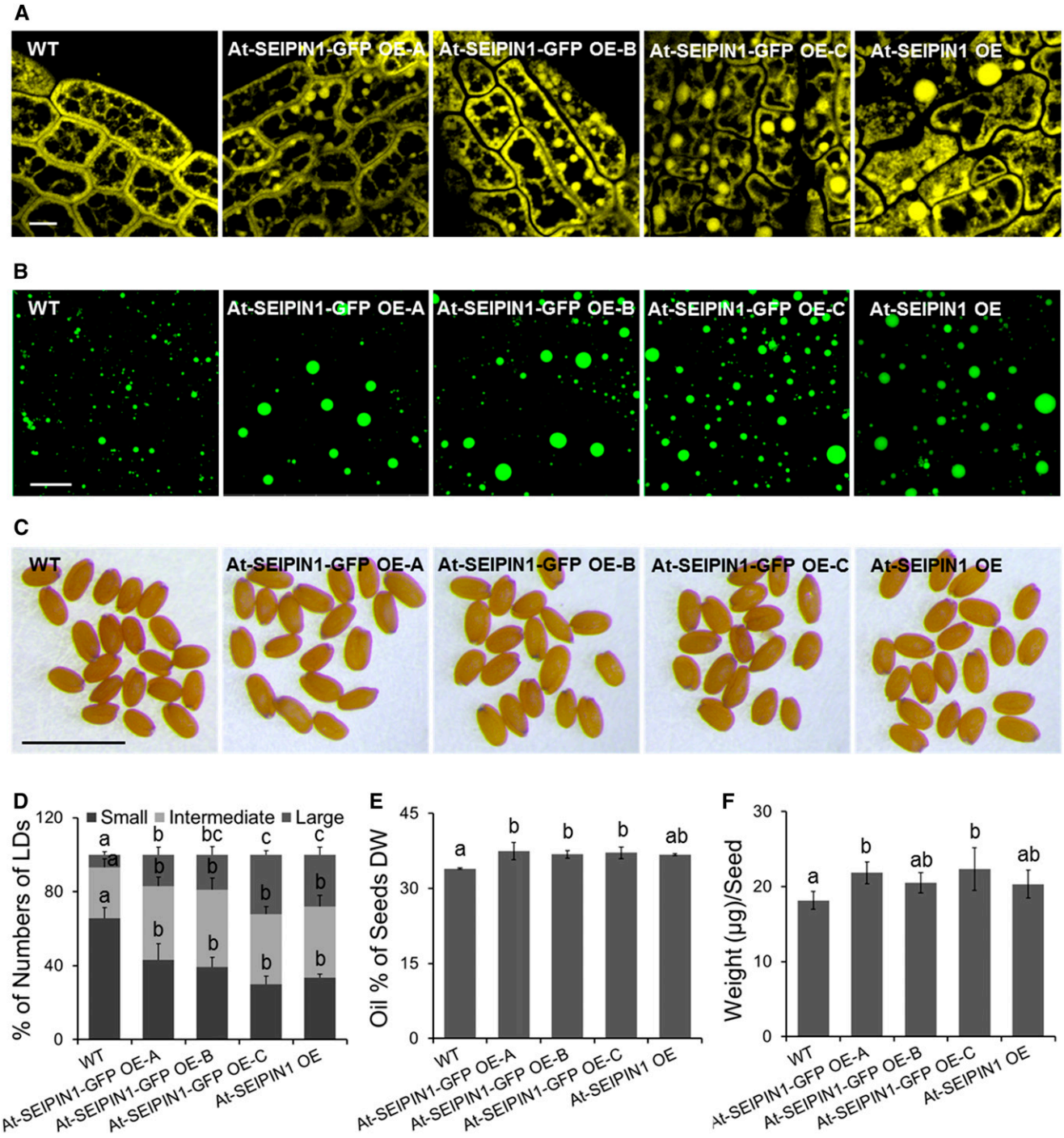

Figure 10. Overexpression of Arabidopsis SEIPINs in Arabidopsis Increases the Size of LDs and Oil Content in Mature Seeds.

(A) Representative confocal images of LDs (Nile Red, yellow) in Arabidopsis seeds. SEIPIN1-GFP OE-A, B, and C are three transgenic events. Images were collected at the same magnification and show a 44.94 × 44.94-μm field of the embryo. Bar = 5 μm.

(B) Isolated LDs (BODIPY 493/503 fluorescence, false color green) from mature Arabidopsis seeds overexpressing Arabidopsis SEIPIN1. Images are Z-stack projections including all LDs in a 134.82 × 134.82-μm field. Bar = 20 μm.

(C) Mature Arabidopsis seeds overexpressing SEIPIN1. Bar = 1 mm.

(D) Percentage of numbers of different sized LDs isolated from the seeds of wild-type Arabidopsis and SEIPIN1 overexpressing lines. Small LDs, diameters <1.5 μm; intermediate LDs, diameters between 1.5 and 3 μm; large LDs, diameters larger than 3 μm. Values are averages and SD of three individual

number of smaller-sized LDs, more similar to those in cells expressing the yeast *SEIPIN* homolog (Figure 2; Supplemental Figure 6) or the human *SEIPIN* homolog (Szymanski et al., 2007). Similarly, in plant cells, SEIPIN1 appeared to facilitate the formation of larger-sized LDs, while SEIPIN2 and especially SEIPIN3 supported the formation of smaller-sized LDs (Figures 4, 5, and 7), suggesting that there are functionally distinct differences in the Arabidopsis SEIPIN proteins in regards to their role in LD biogenesis, particularly for SEIPIN1 in comparison to SEIPIN2 and SEIPIN3.

The primary amino acid sequences of SEIPIN2 and SEIPIN3 were more similar to each other than to SEIPIN1, yet there were several common motifs among plant, yeast, and human SEIPINs (Figures 1A and 1B; Supplemental Data Set 1 and Supplemental Figures 1 to 4). The precise mechanism of SEIPIN action has been difficult to ascertain, but the yeast protein appears to organize as an oligomer in the ER membrane, specifically at ER-LD junctions, where it is proposed to function as a "vent" for the release of storage lipids from within the ER bilayer (Binns et al., 2010; Cartwright and Goodman, 2012). Recent mutagenesis studies identified a 14-amino acid stretch at the N terminus of yeast SEIPIN that when removed resulted in aberrant, large LDs and improper release of LDs from the ER (Cartwright et al., 2015). Our studies examining the N termini of the Arabidopsis SEIPINs (Figure 8; Supplemental Figure 10) allowed us to extend this concept further, such that the N terminus of SEIPIN3 was determined to be sufficient to change SEIPIN1 from a large-sized LD-forming protein into one that preferentially produces small-sized LDs, similar to native SEIPIN3. Conversely, removing the N terminus of SEIPIN3 or swapping the short N terminus of SEIPIN1 with that of SEIPIN3 converted the truncated or shorter fusion protein into a large-sized LD-forming protein. Hence, plants may have evolved different types of SEIPINs through modification of the N terminus to accommodate different cellular needs for LD release from the ER depending on the plant tissue type and/or developmental stage.

When *SEIPIN1* was stably overexpressed in Arabidopsis, developing embryos accumulated many super-sized LDs. Given that algae contain just a single copy of *SEIPIN*, while all higher plants have at least one *SEIPIN1*-type gene and one or more *SEIPIN2/3*-type gene (Figure 1C), we propose that *SEIPIN1* evolution might have been driven in part by an advantage conferred in packaging large amounts of storage oil in developing seeds, which would enhance plant growth during seedling establishment. That is, SEIPIN1 seems to function as a hyperactive "vent" to accommodate the large flux of TAG in seed tissues during oil biosynthesis, and its ectopic (over) expression in any tissue results in the deposition of relatively larger LDs. On the other hand, *SEIPIN2* and *SEIPIN3* appear to be more constitutively expressed in plant tissues (Supplemental Figure 11) and thus may function more generally in various plant cell types to form LDs for purposes other than for seed storage reserves. In support of this concept, up- or downregulation of *SEIPIN1* expression in Arabidopsis resulted in more or less TAG accumulation per seed, respectively (Figures 9 to 11). However, it has not been possible to date to identify plants with a complete loss of *SEIPIN1* expression, perhaps because it may be essential. Our experiments to manipulate *SEIPIN1* expression in planta demonstrate the involvement of SEIPIN1 in LD formation in seed tissues.

Perhaps nearly as striking as the large LDs generated by SEIPIN1, are the very small-sized LDs generated by SEIPIN3 in *N. benthamiana* leaves. In both instances, large LDs with SEIPIN1 versus small LDs with SEIPIN3, the total TAG was increased in tissues and the fatty acid composition of TAGs was altered. These changes in fatty acid composition included an increase in 16:0 acyl moieties and a reduction in 18:3, but the altered compositions were similar for both large (SEIPIN1) and small (SEIPIN3) LDs. It has been suggested that the accumulation of neutral lipids and a shift in fatty acid composition may influence the numbers and sizes of LDs (Fei et al., 2011b, 2011c; Krahmer et al., 2011; Pol et al., 2014; Vanhercke et al., 2014). However, in this study, the fatty acid composition of TAGs, when elevated by SEIPIN(s) and/or LEC2 induction, were similar, and this was independent of LD size, suggesting that at least in plant leaves, large variations in LD size are not attributable to TAG acyl composition. Instead, our results could be explained by the "push-pull-protect" theory (Vanhercke et al., 2014), in which the formation of LDs "pulls" TAG out of the lipid synthesis reservoir and promotes the accumulation of more acyl groups into TAG at the ER. At-SEIPINs might therefore be viewed, as suggested previously (Cartwright and Goodman, 2012; Cartwright et al., 2015), as release valves at the ER for sequestering and channeling TAG into LDs independent of acyl composition and that the various SEIPINs may differ in their release mechanisms to assemble LDs of distinct sizes.

Undoubtedly, it will be interesting to determine if the SEIPINs rely on other cellular proteins to help regulate LD size and whether the various SEIPINs recruit different proteins, or perhaps a different stoichiometry of similar proteins, during LD biogenesis. It is also possible that the multiple SEIPINs in plants might have additional, undiscovered functions in lipid metabolism, lipid trafficking, or membrane fusion. Notably, additional proteins have been identified in yeasts and mammals that work in concert with SEIPIN to influence LD size (Yang et al., 2012; Wilfling et al., 2014), and while some of these genes have distantly related homologs in plants, many others have no apparent plant homologs (Chapman et al., 2012). Thus, there are likely to be organism-specific and possibly variations on the mechanistic themes for LD biogenesis, including the regulation of LD size. For instance, a recent study in yeast identified a protein called

Figure 10. (continued).

experiments (more than 100 LDs were measured for each sample in each individual experiment). Different letters indicate significant difference at $P < 0.05$, as determined by one-way ANOVA with Tukey's post-test.

(E) Percentage of oil in dry seeds. Values are averages and SD of three individual measurements on 50 mg/sample. Seeds were harvested from plants grown under identical conditions, and trends of increased oil content in SEIPIN transgenics were observed in three independent growth trials. Different letters indicate significant difference at $P < 0.05$, as determined by one-way ANOVA with Tukey's post-test.

(F) Average seed weight. Values are averages and SD of seeds harvested from six individual plants. Different letters indicate significant difference at $P < 0.05$, as determined by one-way ANOVA with Tukey's post-test.

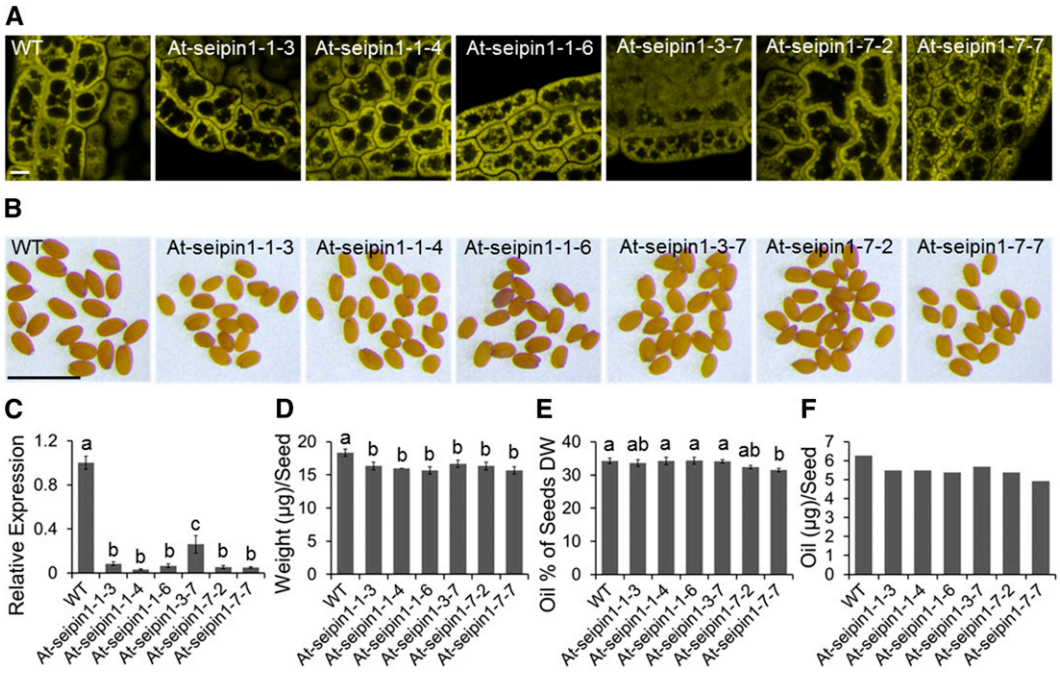

Figure 11. Downregulation of *SEIPIN1* in Arabidopsis by RNAi Decreases the Seed Size and Oil Content per Seed.

Six RNAi lines presented here are from three different transgenic events. seipin1-1-3, seipin1-1-4, and seipin1-1-6 are three lines from the same transgenic event, seipin1-1. seipin1-3-7 is from transgenic event seipin1-3. seipin1-7-2 and seipin1-7-7 are two lines from the same transgenic event, seipin1-7.

(A) Representative confocal images of LDs (Nile Red, yellow) in Arabidopsis seeds. Bar = 5 μm.

(B) Mature Arabidopsis seeds with down-regulated *SEIPIN1*. Bar = 1 mm.

(C) Relative expression level of *SEIPIN1* in RNAi lines assessed by RT-qPCR. Values are averages and SD of three replicates. Different letters indicate significant difference at $P < 0.05$, as determined by one-way ANOVA with Tukey's post-test.

(D) Average seed weight. Seeds were harvested from plants grown under identical conditions, and trends of decreased seed weight were observed in all six RNAi lines. Values are averages and SD of three individual measurements of 100 seeds/replicate. Different letters indicate significant difference at $P < 0.05$, as determined by one-way ANOVA with Tukey's post-test.

(E) Oil percentage of seed dry weight. Values are averages and SD of three individual measurements on 50 mg/sample. Different letters indicate significant difference at $P < 0.05$, as determined by one-way ANOVA with Tukey's post-test.

(F) Oil content per seed. Values are calculated by multiplying oil percentage of seeds' dry weight by average seed weight.

Ldb16 that physically interacts with yeast SEIPIN to support LD biogenesis (Wang et al., 2014). Interestingly, loss of Ldb16 function in yeast could be functionally complemented by overexpression by human SEIPIN, but not by yeast SEIPIN, suggesting that human SEIPIN adopts an architecture similar to the Ldb16-yeast SEIPIN complex to regulate LD size and production (Wang et al., 2014). Therefore, it will be interesting to further explore the functional and mechanistic aspects of SEIPINs, including the plant SEIPINs, as well as any related proteins, to elucidate the details (and variations thereof) of LD biogenesis in eukaryotic cells in general. There are many working models explaining how LDs are produced and expanded at the ER, and the two most widely accepted mechanisms for LD growth are (1) targeted delivery and (2) local synthesis of TAGs (Yang et al., 2012; Pol et al., 2014). In the former model, nascent LDs remain tethered to the ER as they are filled with TAG and other neutral lipid components, and the lipid-synthesizing enzymes are sequestered into lipid-synthesizing subdomains of ER to efficiently supply lipids for LD filling and expansion. Thereafter, the mature LD is released into the cytosol (Shockey et al., 2006; Jacquier et al., 2011; Brasaemle and Wolins, 2012; Xu et al., 2012; Yang et al., 2012; Pol et al., 2014). The local synthesis model, on other hand, suggests that lipids are synthesized on the existing, detached LDs by enzymes that are targeted to the LDs after their release from the ER into the cytosol (Yang et al., 2012; Wilfling et al., 2013; Pol et al., 2014). These two models are not mutually exclusive, and it is likely that, depending on species, developmental stage, and/or tissue type, both mechanisms participate to varying degrees in LD biogenesis in eukaryotes. Our results with the transient expression of SEIPINs in tobacco leaves and by extension in stably transformed Arabidopsis plants could be interpreted to indicate that SEIPINs participate in the organization of ER subdomains that are devoted to TAG synthesis and LD formation (Figures 7 and 9; Supplemental Movies 1 to 6). For instance, SEIPINs colocalized with ER and LDs at discrete subcellular locations in leaf cells, suggesting that ER was repurposed in large measure to synthesize TAG and LDs. Certainly, the ectopic (over)expression of individual SEIPINs in the tobacco leaf system is an artificial situation and should be interpreted with caution. Nonetheless, the consistency of reorganization of the ER and manipulation of LD biogenesis by these SEIPIN proteins in three different eukaryotic systems (yeast cells and leaves of two different plant species) suggest that we are

observing a process that is exaggerated in these heterologous systems rather than simply a subcellular artifact of ectopic (over) expression. Furthermore, sampling during earlier time points of expression of SEIPINs in tobacco leaves revealed what appeared to be specific regions of the ER (subdomains) involved in the early stages of LD biogenesis (Supplemental Figure 9). It should also be emphasized that the *N. benthamiana* system has been valuable to identify enzymes involved in lipid metabolism (Petrie et al., 2010), and here we show that this transient system provides a plant tissue context for evaluating cellular processes like LD biogenesis. Still and as mentioned above, it will be important to identify additional proteins associated with plant SEIPINs that participate in the formation and expansion of LDs to develop a more detailed model of LD biogenesis in plant cells.

The ability to control the number and size of LDs independent of tissue context may have practical value. Efforts are underway by many laboratories to engineer increases in oil content in vegetative tissues of plants (Santos Mendoza et al., 2005; Durrett et al., 2008; Vanhercke et al., 2014). Elevating the lipid content of plant tissues would increase the energy density of these tissues and provide additional biomass for bioenergy applications or energy-dense animal feeds (Durrett et al., 2008; Chapman and Ohlrogge, 2012; Chapman et al., 2013). Expression of SEIPINs in tobacco leaves more than doubled the TAG levels in vegetative tissues, similar to expression of a seed-specific transcription factor, LEC2 (Figures 6A and 6B), suggesting that SEIPINs may be good targets for manipulating the oil content, especially in vegetative tissues of crop plants. Indeed, stable overexpression of *SEIPIN1* increased the LD numbers in Arabidopsis leaves in a manner similar to that in tobacco leaves (Figure 9; Supplemental Figure 12). In addition, and as an unanticipated bonus, the transgenic plants expressing Arabidopsis SEIPIN1 possessed an increase in seed oil content that accompanied an increase in average LD size in embryos (Figure 10). It therefore seems that SEIPIN1 influences the size and amount of TAG-containing LDs when ectopically expressed in vegetative tissues and in seed tissues, raising the possibility that the process of LD formation could be an attractive target for elevating TAG accumulation in plants in general. Moreover, manipulation of LD size makes possible the packaging of lipophilic compounds into various-sized compartments in vivo, which may be desirable for the production of specialty compounds that can be enriched in selective-sized LDs. Certainly, approaches to engineer lipid pathways in crop plants will benefit from a better understanding of how lipids are compartmentalized, and our results provide evidence for a player in plant systems.

METHODS

Plant Materials

Arabidopsis thaliana (Columbia-0) plants used for gene isolation and seed characterization were maintained in chambers at 21°C with a 16:8 h light: dark cycle and 50 $\mu E \cdot m^2 \cdot s$ light intensity. Arabidopsis plants used for LD visualization were grown on half-strength Murashige and Skoog medium plates without sucrose. For analysis of seed parameters, T2 or T3 homozygous plants were identified by segregation analysis and sown in soil. All plants for each analysis were grown at the same time under identical conditions. *Nicotiana benthamiana* plants used for transient expression were grown in soil at 28°C with a 10:14 h light:dark cycle.

Yeast Strains and Growth Conditions

Wild-type yeast strain (BY4742), *SEIPIN* deletion yeast mutant (*ylr404wΔ*), and yeast expression plasmids (pRS315-PGK and pRS315-Sc-*SEIPIN*) were previously described (Szymanski et al., 2007). Yeast cells for microscopy and lipid analysis were grown in appropriate synthetic complete (SC) dropout medium (with glucose or oleic acid as a carbon source) at 28°C until early stationary phase (OD ~3.0).

Gene Cloning and Plasmid Construction

The coding regions of *SEIPIN1*, *SEIPIN2*, and *SEIPIN3* were isolated from wild-type Arabidopsis plants using RT-PCR. RNA was purified using the RNeasy Plant Mini Kit (Qiagen), and samples were treated by DNase (Promega) to avoid DNA contamination. About 100 ng total RNA from each sample was used for RT-PCR, which was performed using the SuperScript One-Step RT-PCR system (Invitrogen). Appropriate forward and reverse primers used to amplify coding regions of *SEIPIN1*, *SEIPIN2*, and *SEIPIN3* were S1FP1/S1RP1, S2FP1/S2FP1, and S3FP1/S3RP1, respectively (Supplemental Table 1). The RT-PCR program was set up as follows, reverse transcription at 42°C for 15 min, predenaturation at 95°C for 5 min, 35 amplification cycles (94°C for 30 s, 50°C for 30 s, and 72°C for 90 s), and postextension step at 72°C for 7 min. Thereafter, each of the cloned coding regions of Arabidopsis *SEIPIN* genes was inserted into binary vectors pMDC32, pMDC43, and pMDC84 (Curtis and Grossniklaus, 2003) using restriction enzymes *Asc*I and *Pac*I (Promega) to construct plant expression plasmids.

To express Arabidopsis SEIPINs in yeast, the cloned coding regions of *SEIPIN1*, *SEIPIN2*, and *SEIPIN3* were inserted into yeast expression vector pRS315-PGK using restriction enzymes *Bam*HI and *Pst*I (Promega). Plant expression plasmids pORE04-*LEC2* and pORE04-*P19* were provided by Qing Liu from CSIRO Plant Industry, Australia (Petrie et al., 2010). Domain-swapped/truncated *SEIPIN*s were generated using PCR fusion cloning procedures (Atanassov et al., 2009) and then subcloned into binary vector pMDC84 (Curtis and Grossniklaus, 2003) using restriction enzymes *Asc*I and *Pac*I. The primers used to clone domain-swapped At-*SEIPIN1N-3C* were S1NFP, S1NARP, S3CAFP, and S3CRP (Supplemental Table 1). The primers used to generate domain-swapped At-*SEIPIN3N-1C* were S3NFP, S3NARP, S1CAFP, and S1CRP (Supplemental Table 1). The primer pairs used to clone N-terminal truncated At-*SEIPIN3-NΔ*, wild-type Sc-*SEIPIN*, and N-terminal truncated Sc-*SEIPIN-NΔ* were S3TAFP/S3CRP, SYFP/SYRP, and SYTFP/SYRP, respectively (Supplemental Table 1). To silence *SEIPIN1* in Arabidopsis, an artificial microRNA construct was designed against the sequence of *SEIPIN1* using the online program Web MicroRNA Designer (http://wmd3.weigelworld.org/cgi-bin/webapp.cgi). The sequence of the target site is 5′-TGTAACATACAAGGTCGGCTC-3′. The *SEIPIN1*-specific microRNA was cloned from the vector pRS300 containing miR319a precursor as described by Schwab et al. (2006). Primers used to clone the *SEIPIN1*-specific microRNA were S1D-miR1, S1D-miR2, S1D-miR3, S1D-miR4, Oligo-miR-A, and Oligo-miR-B (Supplemental Table 1). The cloned *SEIPIN1*-specific microRNA was then inserted into the binary vector pMDC32 (Curtis and Grossniklaus, 2003) using restriction enzymes *Asc*I and *Pac*I (Promega).

Phylogenetic Analysis

The polypeptide sequences of various SEIPIN proteins were identified using the "Protein Homologs" tool available at Phytozome.net (database version 9.1; www.phytozome.net; Goodstein et al., 2012). Briefly, a BLASTP search of the Arabidopsis proteome was conducted using SEIPIN1 as a query to ensure that all three Arabidopsis SEIPINs were identified. From the Web page of the *SEIPIN1* gene, the "Protein Homologs" tool was used to identify all homologous proteins encoded by genes in organisms whose genomes had been sequenced. A subset of this list

was generated by selecting sequences present in either algae or a representative plant from all the major plant orders. The polypeptide sequences within a given plant species were carefully evaluated to eliminate potential duplicates. The phylogenetic relationships of the polypeptide sequences were subsequently analyzed using the one-click Web interface available at phylogeny.fr, using default settings (http://www.phylogeny.fr; Dereeper et al., 2008, 2010). The figure was composed using Adobe Illustrator (version CS6).

Yeast Transformation and Selection of Transformed Cells

The yeast expression plasmids (pRS315-At-*SEIPIN*1, pRS315-At-*SEIPIN2*, pRS315-At-*SEIPIN3*, and pRS315-Sc-*SEIPIN*) were transformed into *SEIPIN* deletion yeast mutant (*ylr404wΔ*) using the Frozen-EZ Yeast Transformation II kit (Zymo Research). The transformed yeast cells were selected by growth on appropriate SC dropout medium (SC-LEU) and further confirmed by PCR. The plasmids in transformed yeast cells were extracted using the ChargeSwitch Plasmid Yeast Mini Kit (Invitrogen) and used as the templates in PCR reactions with GoTaq DNA polymerase (Promega). The PCR program was the same as that that used for subcloning except the extension temperature was 72°C instead of 68°C.

Agrobacterium tumefaciens-Mediated Transient Expression in *N. benthamiana* Leaves

The recombined plant expression plasmids were transformed into Agrobacterium (GV3101) by electroporation. Agrobacteria containing appropriate binary vectors were mixed and diluted with infiltration buffer to make the final mixtures used to infiltrate *N. benthamiana* leaves. The recipe of infiltration buffer, Agrobacterium growth conditions, and infiltration procedures were previously described by Petrie et al. (2010). Expression of the tomato bushy stunt virus gene *P19* was included in all infiltration mixtures to enhance the transformed cDNA expression in *N. benthamiana* leaf tissue (Voinnet et al., 2003; Petrie et al., 2010). *LEC2* in pORE04 vector was included in appropriate infiltration mixtures to enhance the synthesis of TAG and to help simulate seed cellular physiology in *N. benthamiana* leaf tissues (Petrie et al., 2010). The expression of the transformed cDNA(s) in *N. benthamiana* leaf tissue was confirmed at the transcriptional level using RT-PCR (Supplemental Figure 7). RNA was purified from *N. benthamiana* leaf tissue by the RNeasy Plant Mini Kit (Qiagen) and treated by DNase (Promega) to avoid DNA contamination. RT-PCR was performed using the One-Step Ex Tag RT-PCR kit (Takara). Fifty nanograms of total RNA was used in each RT-PCR. The reverse transcription step included incubation at 42°C for 15 min. The predenaturation step was at 95°C for 5 min. The postextension step was at 72°C for 7 min. Nb-*EF1α* and *P19* were amplified by 35 cycles with 94°C for 30 s, 55°C for 30 s, and 72°C for 30 s. *LEC2* and *SEIPIN1* were amplified by 35 cycles with 94°C for 30 s, 50°C for 30 s, and 72°C for 1 min. *SEIPIN2* and *SEIPIN3* were amplified by 35 cycles with 94°C for 30 s, 50°C for 30 s, and 72°C for 1.5 min. The forward/reverse primers to amplify *SEIPIN1*, *SEIPIN2*, *SEIPIN3*, *LEC2*, Nb-*EF1α*, or *P19* were S1FP2/S1RP2, S2FP2/S2RP2, S3FP2/S3RP2, LEC2FP/LEC2RP, EFFP/EFRP, or P19FP/P19RP, respectively (Supplemental Table 1).

Agrobacterium-Mediated Stable Transformation of Arabidopsis and Expression Analysis

Recombined plasmids pMDC32-*SEIPIN1* and pMDC43-*SEIPIN1* were used to stably express *SEIPIN1* and *SEIPIN1-GFP* in wild-type Arabidopsis (Columbia-0). Agrobacterium-mediated stable transformation in Arabidopsis was performed as described by Clough and Bent (1998). Then, the expression of *SEIPIN1* and *SEIPIN1-GFP* was detected by RT-PCR. RNA extraction from Arabidopsis leaves and RT-PCR were performed as described above for the tobacco transient expression system. At-*EF1α* was used as the control gene expressed in transgenic and nontransgenic tissues and was amplified by 30 cycles with 94°C for 30 s, 55°C for 30 s, and 72°C for 1 min. *SEIPIN1* and *SEIPIN1-GFP* were amplified by 30 cycles with 94°C for 30 s, 50°C for 30 s, and 72°C for 1.5 min. For each reaction, 50 ng of total RNA was used. The forward/reverse primers used for At-*EF1α*, *SEIPIN1*, and *SEIPIN1-GFP* were EF1αFP/EF1αRP, S1FP2/S1RP2, and S1FP2/GFPRP, respectively (Supplemental Table 1).

Recombined plasmid pMDC32-S1D containing the *SEIPIN1*-specific microRNA was transformed into Arabidopsis using the Agrobacterium-mediated floral dip method in an attempt to suppress the expression of *SEIPIN1* in Arabidopsis. The transcript levels of *SEIPIN1* in homozygous Arabidopsis seeds were analyzed using RT-qPCR. About 25 mg of dry seeds per sample was used for RNA extraction, and ~20 ng of RNA was used in each RT-qPCR replicate. The RT-qPCR was performed using the One-Step Ex Tag RT-PCR kit, and the program was set up as reverse transcription at 42°C for 15 min, predenaturation at 95°C for 2 min, and 40 amplification cycles (94°C for 10 s, 60°C for 25 s, and 72°C for 20 s). The primer pairs used to amplify the reference genes At-*EF1α* and *SEIPIN1* were EF1αFP/EF1αRP and S1qFP/S1qRP, respectively (Supplemental Table 1).

To test the expression pattern of the three *SEIPIN* genes in wild-type Arabidopsis (Columbia-0), RT-PCR was performed on RNA isolated from dry seeds, imbibed seeds, seedlings, leaves, flowers, stems, and roots. RNA was extracted using the RNeasy Plant Mini Kit (Qiagen) and treated with DNase (Promega) to remove DNA contamination. RT-PCR was performed using One-Step Ex Tag RT-PCR kit and 20 ng of total RNA per reaction. The PCR program was set up for reverse transcription at 42°C for 15 min, predenaturation at 95°C for 5 min, 28 (for At-*EF1α*) or 35 (for *SEIPIN*s) amplification cycles (94°C for 30 s, 55°C for 30 s, and 72°C for 30 s), and postextension at 72°C for 7 min. The forward/reverse primers to amplify *SEIPIN1*, *SEIPIN2*, *SEIPIN3*, and At-*EF1α* were S1FP2/S1RP2, S2FP2/S2RP2, S3FP2/S3RP2, and EF1αFP/EF1αRP, respectively (Supplemental Table 1).

Lipid Extraction and Analysis

To quantify the TAG content and composition in yeast cells and tobacco leaves, 50 OD_{600} units of yeast cells or 50 mg of dried tobacco leaves was collected for each biological replicate. Yeast cells and tobacco leaves were both disrupted using glass beads and bead beater (BioSpec Mini-Beadbeater-16). For yeast lipid samples, 5 μg TAG (tri-15:0) standard was added into each sample before extraction. Total lipid was extracted using hot (70°C) isopropanol and chloroform in a ratio of 450 mg sample:2 mL isopropanol:1 mL chloroform at 70°C for 30 min and then at 4°C overnight. Then the total lipid was further purified by adding 1 mL chloroform and 2 mL 1 M KCl, followed by washing with 2 mL 1 M KCl twice. The purified lipid was dried under N_2 and stored in 400 μL 1:1 chloroform/methanol at −20°C. The neutral lipid was separated from polar lipid using solid-phase extraction. The column used in solid-phase extraction was a 6-mL silica column (Sigma-Aldrich). Five milliliters of hexane/diethyl ether 4:1 and 5 mL of hexane/diethyl ether 1:1 were used to elute neutral lipids for yeast lipid samples, and 5 mL of hexane/diethyl ether 4:1 was used to elute neutral lipids for tobacco leaf samples. The neutral lipid and polar lipid samples were evaporated under nitrogen and redissolved in chloroform/methanol 1:1 for storage. TAG content and composition in yeast cells was quantified by electrospray ionization triple quadrupole mass spectrometry (Thermo TS Quantum). The spectrum was acquired using Xcalibur (v.2.0.7) and processed by Metabolite Imager (v.1.0) to quantify the total amount and composition of TAG. Neutral lipids from tobacco leaves were separated by TLC (as described in James et al., 2010) and visualized with 0.005% primulin spray under UV light (White et al., 1998). Standard curves were generated with known neutral lipid standards that were separated on TLC places and compared with tobacco neutral lipid classes on TLC plates for relative quantification by densitometry using ImageJ. A neutral lipid standard mixture was cochromatographed with the tobacco neutral lipid fractions to confirm the appropriate relative mobility and to ensure that

lipids were present within the range of the standard curve. Additionally, a portion of each total neutral lipid fraction was transesterified in methanolic HCl, and the fatty acids in neutral lipids were quantified using gas chromatography-flame ionization detection (Agilent, HP 5890) with heptadecanoic acid as an internal standard. Methods and conditions for electrospray ionization-triple quadrupole mass spectrometry and gas chromatography-flame ionization detection were as described by James et al. (2010). Lipid and fatty acid standards were purchased from Nu-Chek Prep. The oil content in Arabidopsis desiccated seeds was quantified by time-domain, pulse-field ^{1}H-NMR on a Bruker minispec mq20 (Bruker Optics). Approximately 50 mg of dry seeds was used for each measurement, and oil was quantified according to Chapman et al. (2008), except that the instrument was calibrated for Arabidopsis seeds.

Visualization and Analysis of LDs

To visualize LDs in yeast cells, *N. benthamiana* leaves, and Arabidopsis, LDs were stained with 0.4 μg/mL (for yeast) or 2 μg/mL (for tobacco leaves) BODIPY 493/503 (Invitrogen; from 4 mg/mL stock in DMSO) or 2 μg/mL (for Arabidopsis leaves and seeds) Nile Red (Sigma-Aldrich; from 1 mg/mL stock in DMSO) in 50 mM PIPES buffer (pH 7.0). For Arabidopsis leaves, the sixth rosette leaf of 4-week-old plants was used for LD visualization and analysis. Confocal images were acquired using a Zeiss LSM710 confocal laser scanning microscope. BODIPY 493/503 was excited by a 488-nm laser, and the emission signal was collected in a spectrum of 500 to 540 nm. Nile Red was excited by a 488-nm laser, and the emission was acquired from 560 to 620 nm. Both 2D images and Z-stack projections were saved as 512 × 512-pixel (for yeast) and 1024 × 1024-pixel (for tobacco leaves and Arabidopsis) images. To further verify the LD phenotype, TEM was used to image the LDs in yeast cells and Arabidopsis seeds. The yeast cells were fixed, embedded and stained as described (Wright, 2000). Arabidopsis seeds were fixed in 30 mM HEPES NaOH buffer, pH 7.4, containing 4% paraformaldehyde and 2.5% glutaraldehyde, and microwave pulses (6 cycles of 30 s, 1500 watts, on ice) were applied to assist penetration of fixatives. Osmium tetroxide (1% by volume) was used for postfixation. The fixed seeds were dehydrated through a graded ethanol series and then embedded in LR white resin (Electron Microscopy Sciences). Embedded seeds were incubated at 55°C for 2 d to promote polymerization. Polymerized blocks containing yeast cells or Arabidopsis seeds were cut into ultrathin sections using an ultramicrotome (RMC MT6000 or Leica Ultracut UCT), and sections of seeds were poststained with 2% uranyl acetate and Reynolds' lead citrate. Images were collected using either a Philips EM420 TEM or FEI Tecnai G2 F20.

Numbers and sizes of LDs were quantified using ImageJ 1.43t. In yeast, Z-stack projections including all cells in particular areas were used for quantification. More than 150 cells for each strain from at least three separate transformations were used for numerical quantification, and 30 cells for each strain were analyzed for LD size quantification. Z-stack projections were used for numerical quantification. The sizes of LDs in *N. benthamiana* and Arabidopsis leaves were indicated as average diameters. For LDs in *N. benthamiana*, nine 2D images from three individual experiments for each infiltration were used to quantify the number of LDs for different size categories. In Arabidopsis leaves, nine Z-stack series from three plants for each genotype were used to quantify the LDs in different size categories. The sixth leaf from the bottom was used for LD visualization and quantification in each Arabidopsis plant. All the significance tests performed in this study were determined by one-way ANOVA with Tukey's post-test.

Visualization of ER and Colocalization of ER, LDs, and Arabidopsis SEIPINs

ER in yeast cells and tobacco leaves was labeled using the ER marker protein Kar2-CFP-HDEL (Szymanski et al., 2007) and imaged by confocal laser scanning microscopy (Zeiss LSM710). Arabidopsis SEIPINs were localized by fusing GFP at the N or C terminus of each SEIPIN protein. LDs were stained as described above. Confocal images were acquired using a Zeiss LSM710 confocal laser scanning microscope. GFP was excited by a 488-nm laser, and the emission signal was collected in a spectrum of 500 to 540 nm. CFP was excited by a 405-nm laser, and the fluorescent signal was collected from 450 to 490 nm. Nile Red was excited by a 488-nm laser, and the emission was acquired from 560 to 620 nm. Chloroplast autofluorescence was collected in an emission spectrum of 640 to 720 nm.

Isolation and Visualization of LDs from Arabidopsis Seeds

To isolate LDs from Arabidopsis seeds by flotation centrifugation (Chapman and Trelease, 1991), 2 mg of dry seeds for each sample was imbibed in water for 15 min to soften the seed coat, then the seeds were homogenized in sucrose/Tris-HCl buffer (500 mM sucrose in 100 mM Tris-HCl, pH 7.5). The homogenate was transferred to a 15-mL Corex high-speed centrifuge tube and 1 mL of 1 M Tris-HCl, pH 7.5, was layered on the top of the homogenate. Samples were centrifuged at 10,500*g* (Sorvall SS34 rotor; Sorvall RC 5C high-speed centrifuge) for 60 min at 4°C. The cloudy looking lipid pad on the top of the tube was collected for staining and visualization. All samples were kept on ice during LD isolation to minimize LD fusion. BODIPY 493/503 (0.4 mg/mL; Invitrogen; from 4 mg/mL stock in DMSO) in 50 mM PIPES buffer (pH 7.0) was used to stain the isolated LDs, and confocal images were taken on the same day using a Zeiss LSM710 confocal laser scanning microscope. All images were collected as Z-stack series and were saved as 1024 × 1024-pixel images. The confocal images were used to estimate the size of isolated LDs with equivalent X, Y, and Z dimensions. Three individual isolations were performed for each genotype, and more than 100 LDs were measured for each replicate.

Accession Numbers

Sequence data from this article can be found in the GenBank/EMBL data libraries under accession numbers AED92296 (At-*SEIPIN1*), AEE31126 (At-*SEIPIN2*), AEC08966 (At-*SEIPIN3*), AAH04911 (human *SEIPIN*), and CAY81629 (yeast *SEIPIN*). The Arabidopsis Genome Initiative locus identifiers are At5g16460 (*SEIPIN1*), At1g29760 (*SEIPIN2*), and At2g34380 (*SEIPIN3*). Additional polypeptide sequences used for phylogenetic analysis, including their Phytozome accession numbers, are as follows: *A. coerulea*-1, Aquca_003_00537.1; *A. coerulea*-2, Aquca_039_00023.1; *A. coerulea*-3, Aquca_021_00111.1; *C. sinensis*-1, orange1.1g041179m; *C. sinensis*-2, orange1.1g010745m; *C. subellipsoidea*, 45808; *F. vesca*-1, mrna16808.1-v1.0-hybrid; *F. vesca*-2, mrna23792.1-v1.0-hybrid; *F. vesca*-3, mrna00278.1-v1.0-hybrid; *F. vesca*-4, mrna27316.1-v1.0-hybrid; *G. raimondii*-1, Gorai.012G028100.1; *G. raimondii*-2, Gorai.010G240300.1; *G. raimondii*-3, Gorai.011G035700.1; *M. pusilla*, 63945; *M. truncatula*-1, 30,026.m001489; *M. truncatula*-2, Medtr2g017670.1; *M. truncatula*-3, Medtr8g087730.1; *O. lucimarinus*, 30523; *P. patens*-1, Pp1s325_14V6.1; *P. patens*-2, Pp1s96_232V6.1; *R. communis*-1, 29,929.m004585; *R. communis*-2, 30,026.m001489; *S. lycopersicum*-1, Solyc04g056380.2.1; *S. lycopersicum*-2, Solyc02g071900.2.1; *S. lycopersicum*-3, Solyc07g062230.2.1; *V. vinifera*-1, GSVIVT01019108001; *V. vinifera*-2, GSVIVT01021275001; *V. vinifera*-3, GSVIVT01014151001; *Z. mays*-1, GRMZM2G051697_T02; and *Z. mays*-2, GRMZM2G147454_T01.

Supplemental Data

Supplemental Figure 1. Deduced polypeptide sequence alignment of SEIPIN homologs in yeast, human, and Arabidopsis.

Supplemental Figure 2. Deduced polypeptide sequence alignment of SEIPIN homologs in Arabidopsis.

Supplemental Figure 3. Amino acid sequences of various motifs shared between SEIPINs in yeast, humans, and Arabidopsis.

Supplemental Figure 4. Amino acid sequences of various motifs shared between the three Arabidopsis SEIPINs.

Supplemental Figure 5. Representative electron micrographs of LDs in wild-type yeast, yeast *SEIPIN* deletion mutant (*ylr404w*Δ), and yeast *SEIPIN* deletion mutant expressing individual Arabidopsis SEIPINs.

Supplemental Figure 6. Complementation tests for LD phenotypes in the yeast *SEIPIN* deletion mutant (*ylr404w*Δ, fed with oleic acid) by Arabidopsis SEIPINs compared with functional complementation with yeast SEIPIN.

Supplemental Figure 7. Confirmation of the expression of Arabidopsis SEIPINs in tobacco leaves using qualitative RT-PCR.

Supplemental Figure 8. Colocalization of LD and Arabidopsis SEIPINs in tobacco leaves.

Supplemental Figure 9. Phenotypes of ER organization and LDs at 3 days after infiltration of SEIPIN1 or SEIPIN3.

Supplemental Figure 10. Localization of domain-swapped/truncated Arabidopsis and yeast SEIPINs in tobacco leaves.

Supplemental Figure 11. Analysis of expression patterns of Arabidopsis *SEIPIN* genes in different tissues and developmental stages by RT-PCR.

Supplemental Figure 12. Expression and localization of SEIPIN1 in Arabidopsis leaves.

Supplemental Figure 13. Representative electron micrographs of LDs in wild-type and SEIPIN1-overexpressing Arabidopsis seeds.

Supplemental Table 1. Names and sequences of primers used in this study.

Supplemental Data Set 1. Alignments used to generate the phylogeny presented in Figure 1C.

Supplemental Movie 1. ER and LDs in tobacco leaves with the absence of SEIPIN.

Supplemental Movie 2. Colocalization of GFP-tagged SEIPIN1, ER, and LDs in tobacco leaves.

Supplemental Movie 3. Colocalization of GFP-tagged SEIPIN2, ER, and LDs in tobacco leaves.

Supplemental Movie 4. Colocalization of GFP-tagged SEIPIN3, ER, and LDs in tobacco leaves.

Supplemental Movie 5. Colocalization of GFP-tagged SEIPINs, ER, and LDs in tobacco leaves expressing all three SEIPINs.

Supplemental Movie 6. Colocalization of GFP-tagged SEIPIN1 and LDs in Arabidopsis leaves.

ACKNOWLEDGMENTS

This research was supported by a grant from the U.S. Department of Energy, Division of Biological and Environmental Research (DE-FG02-09ER64812/DE-SC0000797). The Zeiss LSM710 confocal laser scanning microscope was acquired with funds from NSF-MRI Grant 1126205 to the University of North Texas (UNT). We thank Derk Binns at the University of Texas Southwestern Medical Center, Dallas, TX, for the yeast mutant strain *ylr404w*Δ, yeast expression plasmids pRS315-PGK and pRS315-Sc-*SEIPIN*, and advice regarding *SEIPIN* expression in transgenic yeast. We also thank David Garrett (UNT) for performing TEM of yeast cells, Lon Turnbull (UNT) for assistance with the confocal microscope, Bob Harris (Molecular and Cellular Imaging Facility, University of Guelph) for assistance with TEM of Arabidopsis mature seeds, and Qing Liu from CSIRO Plant Industry, Australia, for providing us with plant expression plasmids pORE04-*LEC2* and pORE04-*P19*. K.D.C. is grateful to the National Science Foundation for providing individual research and development leave to assist in the supervision of this research and the preparation of this article by agreement under the Intergovernmental Personnel Act. J.M.G. was supported by funding provided by the National Institutes of Health (Grant R01 GM084210) and the American Diabetes Association (Grant 7-13-BS-055). R.T.M. was supported by funding provided by the Natural Sciences and Engineering Research Council of Canada.

AUTHOR CONTRIBUTIONS

Y.C. and M.P. performed experiments. Y.C. and K.D.C. designed experiments. All authors interpreted and evaluated data, suggested additional experiments, and contributed to the writing of the article.

Received July 7, 2015; revised August 12, 2015; accepted August 24, 2015; published September 11, 2015.

REFERENCES

Andrianov, V., Borisjuk, N., Pogrebnyak, N., Brinker, A., Dixon, J., Spitsin, S., Flynn, J., Matyszczuk, P., Andryszak, K., Laurelli, M., Golovkin, M., and Koprowski, H. (2010). Tobacco as a production platform for biofuel: overexpression of Arabidopsis DGAT and LEC2 genes increases accumulation and shifts the composition of lipids in green biomass. Plant Biotechnol. J. **8:** 277–287.

Atanassov, I.I., Atanassov, I.I., Etchells, J.P., and Turner, S.R. (2009). A simple, flexible and efficient PCR-fusion/Gateway cloning procedure for gene fusion, site-directed mutagenesis, short sequence insertion and domain deletions and swaps. Plant Methods **5:** 14.

Bailey, T.L., Boden, M., Buske, F.A., Frith, M., Grant, C.E., Clementi, L., Ren, J., Li, W.W., and Noble, W.S. (2009). MEME SUITE: tools for motif discovery and searching. Nucleic Acids Res. **37:** W202–W208.

Bartz, R., Li, W.H., Venables, B., Zehmer, J.K., Roth, M.R., Welti, R., Anderson, R.G., Liu, P., and Chapman, K.D. (2007). Lipidomics reveals that adiposomes store ether lipids and mediate phospholipid traffic. J. Lipid Res. **48:** 837–847.

Baud, S., and Lepiniec, L. (2010). Physiological and developmental regulation of seed oil production. Prog. Lipid Res. **49:** 235–249.

Bi, J., Wang, W., Liu, Z., Huang, X., Jiang, Q., Liu, G., Wang, Y., and Huang, X. (2014). Seipin promotes adipose tissue fat storage through the ER Ca^{2+}-ATPase SERCA. Cell Metab. **19:** 861–871.

Binns, D., Lee, S., Hilton, C.L., Jiang, Q.X., and Goodman, J.M. (2010). Seipin is a discrete homooligomer. Biochemistry **49:** 10747–10755.

Brasaemle, D.L., and Wolins, N.E. (2012). Packaging of fat: an evolving model of lipid droplet assembly and expansion. J. Biol. Chem. **287:** 2273–2279.

Carman, G.M. (2012). Thematic minireview series on the lipid droplet, a dynamic organelle of biomedical and commercial importance. J. Biol. Chem. **287:** 2272.

Cartwright, B.R., and Goodman, J.M. (2012). Seipin: from human disease to molecular mechanism. J. Lipid Res. **53:** 1042–1055.

Cartwright, B.R., Binns, D.D., Hilton, C.L., Han, S., Gao, Q., and Goodman, J.M. (2015). Seipin performs dissectible functions in promoting lipid droplet biogenesis and regulating droplet morphology. Mol. Biol. Cell **26:** 726–739.

Chapman, K.D., Dyer, J.M., and Mullen, R.T. (2012). Biogenesis and functions of lipid droplets in plants: Thematic review series: lipid droplet synthesis and metabolism: from yeast to man. J. Lipid Res. **53:** 215–226.

Chapman, K.D., Dyer, J.M., and Mullen, R.T. (2013). Commentary: why don't plant leaves get fat? Plant Sci. **207:** 128–134.

Chapman, K.D., Neogi, P.B., Hake, K.D., Stawska, A.A., Speed, T.R., Cotter, M.Q., Garrett, D.C., Kerby, T., Richardson, C.D., Ayre, B.G., Ghosh, S., and Kinney, A.J. (2008). Reduced oil accumulation in cottonseeds transformed with a Brassica nonfunctional allele of a Delta-12 Fatty Acid Desaturase (FAD2). Crop Sci. **48:** 1470–1481.

Chapman, K.D., and Ohlrogge, J.B. (2012). Compartmentation of triacylglycerol accumulation in plants. J. Biol. Chem. **287:** 2288–2294.

Chapman, K.D., and Trelease, R.N. (1991). Acquisition of membrane lipids by differentiating glyoxysomes: role of lipid bodies. J. Cell Biol. **115:** 995–1007.

Clough, S.J., and Bent, A.F. (1998). Floral dip: a simplified method for Agrobacterium-mediated transformation of *Arabidopsis thaliana*. Plant J. **16:** 735–743.

Cui, X., Wang, Y., Meng, L., Fei, W., Deng, J., Xu, G., Peng, X., Ju, S., Zhang, L., Liu, G., Zhao, L., and Yang, H. (2012). Overexpression of a short human seipin/BSCL2 isoform in mouse adipose tissue results in mild lipodystrophy. Am. J. Physiol. Endocrinol. Metab. **302:** E705–E713.

Cui, X., Wang, Y., Tang, Y., Liu, Y., Zhao, L., Deng, J., Xu, G., Peng, X., Ju, S., Liu, G., and Yang, H. (2011). Seipin ablation in mice results in severe generalized lipodystrophy. Hum. Mol. Genet. **20:** 3022–3030.

Curtis, M.D., and Grossniklaus, U. (2003). A gateway cloning vector set for high-throughput functional analysis of genes in planta. Plant Physiol. **133:** 462–469.

Dereeper, A., Audic, S., Claverie, J.M., and Blanc, G. (2010). BLAST-EXPLORER helps you building datasets for phylogenetic analysis. BMC Evol. Biol. **10:** 8.

Dereeper, A., Guignon, V., Blanc, G., Audic, S., Buffet, S., Chevenet, F., Dufayard, J.F., Guindon, S., Lefort, V., Lescot, M., Claverie, J.M., and Gascuel, O. (2008). Phylogeny.fr: robust phylogenetic analysis for the non-specialist. Nucleic Acids Res. **36:** W465–W469.

Durrett, T.P., Benning, C., and Ohlrogge, J. (2008). Plant triacylglycerols as feedstocks for the production of biofuels. Plant J. **54:** 593–607.

Farese, R.V., Jr., and Walther, T.C. (2009). Lipid droplets finally get a little R-E-S-P-E-C-T. Cell **139:** 855–860.

Fei, W., Du, X., and Yang, H. (2011a). Seipin, adipogenesis and lipid droplets. Trends Endocrinol. Metab. **22:** 204–210.

Fei, W., Li, H., Shui, G., Kapterian, T.S., Bielby, C., Du, X., Brown, A.J., Li, P., Wenk, M.R., Liu, P., and Yang, H. (2011b). Molecular characterization of seipin and its mutants: implications for seipin in triacylglycerol synthesis. J. Lipid Res. **52:** 2136–2147.

Fei, W., Shui, G., Gaeta, B., Du, X., Kuerschner, L., Li, P., Brown, A.J., Wenk, M.R., Parton, R.G., and Yang, H. (2008). Fld1p, a functional homologue of human seipin, regulates the size of lipid droplets in yeast. J. Cell Biol. **180:** 473–482.

Fei, W., et al. (2011c). A role for phosphatidic acid in the formation of "supersized" lipid droplets. PLoS Genet. **7:** e1002201.

Gidda, S.K., et al. (2013). Lipid droplet-associated proteins (LDAPs) are involved in the compartmentalization of lipophilic compounds in plant cells. Plant Signal. Behav. **8:** e27141.

Goodstein, D.M., Shu, S., Howson, R., Neupane, R., Hayes, R.D., Fazo, J., Mitros, T., Dirks, W., Hellsten, U., Putnam, N., and Rokhsar, D.S. (2012). Phytozome: a comparative platform for green plant genomics. Nucleic Acids Res. **40:** D1178–D1186.

Herker, E., and Ott, M. (2012). Emerging role of lipid droplets in host/pathogen interactions. J. Biol. Chem. **287:** 2280–2287.

Horn, P.J., James, C.N., Gidda, S.K., Kilaru, A., Dyer, J.M., Mullen, R.T., Ohlrogge, J.B., and Chapman, K.D. (2013). Identification of a new class of lipid droplet-associated proteins in plants. Plant Physiol. **162:** 1926–1936.

Huang, A.H. (1996). Oleosins and oil bodies in seeds and other organs. Plant Physiol. **110:** 1055–1061.

Jacquier, N., Choudhary, V., Mari, M., Toulmay, A., Reggiori, F., and Schneiter, R. (2011). Lipid droplets are functionally connected to the endoplasmic reticulum in *Saccharomyces cerevisiae.* J. Cell Sci. **124:** 2424–2437.

Jacquier, N., Mishra, S., Choudhary, V., and Schneiter, R. (2013). Expression of oleosin and perilipins in yeast promotes formation of lipid droplets from the endoplasmic reticulum. J. Cell Sci. **126:** 5198–5209.

James, C.N., Horn, P.J., Case, C.R., Gidda, S.K., Zhang, D., Mullen, R.T., Dyer, J.M., Anderson, R.G., and Chapman, K.D. (2010). Disruption of the Arabidopsis CGI-58 homologue produces Chanarin-Dorfman-like lipid droplet accumulation in plants. Proc. Natl. Acad. Sci. USA **107:** 17833–17838.

Krahmer, N., Guo, Y., Wilfling, F., Hilger, M., Lingrell, S., Heger, K., Newman, H.W., Schmidt-Supprian, M., Vance, D.E., Mann, M., Farese, R.V., Jr., and Walther, T.C. (2011). Phosphatidylcholine synthesis for lipid droplet expansion is mediated by localized activation of CTP:phosphocholine cytidylyltransferase. Cell Metab. **14:** 504–515.

Magré, J., et al.; BSCL Working Group (2001) Identification of the gene altered in Berardinelli-Seip congenital lipodystrophy on chromosome 11q13. Nat. Genet. **28:** 365–370.

Miquel, M., Trigui, G., d'Andréa, S., Kelemen, Z., Baud, S., Berger, A., Deruyffelaere, C., Trubuil, A., Lepiniec, L., and Dubreucq, B. (2014). Specialization of oleosins in oil body dynamics during seed development in Arabidopsis seeds. Plant Physiol. **164:** 1866–1878.

Murphy, D.J. (2012). The dynamic roles of intracellular lipid droplets: from archaea to mammals. Protoplasma **249:** 541–585.

Park, S., Gidda, S.K., James, C.N., Horn, P.J., Khuu, N., Seay, D.C., Keereetaweep, J., Chapman, K.D., Mullen, R.T., and Dyer, J.M. (2013). The α/β hydrolase CGI-58 and peroxisomal transport protein PXA1 coregulate lipid homeostasis and signaling in Arabidopsis. Plant Cell **25:** 1726–1739.

Petrie, J.R., Shrestha, P., Liu, Q., Mansour, M.P., Wood, C.C., Zhou, X.R., Nichols, P.D., Green, A.G., and Singh, S.P. (2010). Rapid expression of transgenes driven by seed-specific constructs in leaf tissue: DHA production. Plant Methods **6:** 8.

Pol, A., Gross, S.P., and Parton, R.G. (2014). Review: biogenesis of the multifunctional lipid droplet: lipids, proteins, and sites. J. Cell Biol. **204:** 635–646.

Rudolph, M., Schlereth, A., Körner, M., Feussner, K., Berndt, E., Melzer, M., Hornung, E., and Feussner, I. (2011). The lipoxygenase-dependent oxygenation of lipid body membranes is promoted by a patatin-type phospholipase in cucumber cotyledons. J. Exp. Bot. **62:** 749–760.

Santos Mendoza, M., Dubreucq, B., Miquel, M., Caboche, M., and Lepiniec, L. (2005). LEAFY COTYLEDON 2 activation is sufficient to trigger the accumulation of oil and seed specific mRNAs in Arabidopsis leaves. FEBS Lett. **579:** 4666–4670.

Schmid, M., Davison, T.S., Henz, S.R., Pape, U.J., Demar, M., Vingron, M., Schölkopf, B., Weigel, D., and Lohmann, J.U. (2005). A gene expression map of *Arabidopsis thaliana* development. Nat. Genet. **37:** 501–506.

Schmidt, M.A., and Herman, E.M. (2008). Suppression of soybean oleosin produces micro-oil bodies that aggregate into oil body/ER complexes. Mol. Plant **1:** 910–924.

Schwab, R., Ossowski, S., Riester, M., Warthmann, N., and Weigel, D. (2006). Highly specific gene silencing by artificial microRNAs in Arabidopsis. Plant Cell **18:** 1121–1133.

Shockey, J.M., Gidda, S.K., Chapital, D.C., Kuan, J.C., Dhanoa, P.K., Bland, J.M., Rothstein, S.J., Mullen, R.T., and Dyer, J.M. (2006). Tung tree DGAT1 and DGAT2 have nonredundant functions in triacylglycerol biosynthesis and are localized to different subdomains of the endoplasmic reticulum. Plant Cell **18:** 2294–2313.

Szymanski, J., Brotman, Y., Willmitzer, L., and Cuadros-Inostroza, Á. (2014). Linking gene expression and membrane lipid composition of Arabidopsis. Plant Cell **26:** 915–928.

Szymanski, K.M., Binns, D., Bartz, R., Grishin, N.V., Li, W.P., Agarwal, A.K., Garg, A., Anderson, R.G., and Goodman, J.M. (2007). The lipodystrophy protein seipin is found at endoplasmic reticulum lipid droplet junctions and is important for droplet morphology. Proc. Natl. Acad. Sci. USA **104:** 20890–20895.

Tian, Y., Bi, J., Shui, G., Liu, Z., Xiang, Y., Liu, Y., Wenk, M.R., Yang, H., and Huang, X. (2011). Tissue-autonomous function of Drosophila seipin in preventing ectopic lipid droplet formation. PLoS Genet. **7:** e1001364.

Vanhercke, T., et al. (2014). Metabolic engineering of biomass for high energy density: oilseed-like triacylglycerol yields from plant leaves. Plant Biotechnol. J. **12:** 231–239.

Voinnet, O., Rivas, S., Mestre, P., and Baulcombe, D. (2003). An enhanced transient expression system in plants based on suppression of gene silencing by the p19 protein of tomato bushy stunt virus. Plant J. **33:** 949–956.

Wang, C.W., Miao, Y.H., and Chang, Y.S. (2014). Control of lipid droplet size in budding yeast requires the collaboration between Fld1 and Ldb16. J. Cell Sci. **127:** 1214–1228.

White, T., Bursten, S., Federighi, D., Lewis, R.A., and Nudelman, E. (1998). High-resolution separation and quantification of neutral lipid and phospholipid species in mammalian cells and sera by multi-one-dimensional thin-layer chromatography. Anal. Biochem. **258:** 109–117.

Wilfling, F., et al. (2013). Triacylglycerol synthesis enzymes mediate lipid droplet growth by relocalizing from the ER to lipid droplets. Dev. Cell **24:** 384–399.

Wilfling, F., Haas, J.T., Walther, T.C., and Farese, R.V., Jr. (2014). Lipid droplet biogenesis. Curr. Opin. Cell Biol. **29:** 39–45.

Winichayakul, S., Scott, R.W., Roldan, M., Hatier, J.H., Livingston, S., Cookson, R., Curran, A.C., and Roberts, N.J. (2013). In vivo packaging of triacylglycerols enhances Arabidopsis leaf biomass and energy density. Plant Physiol. **162:** 626–639.

Winter, D., Vinegar, B., Nahal, H., Ammar, R., Wilson, G.V., and Provart, N.J. (2007). An "Electronic Fluorescent Pictograph" browser for exploring and analyzing large-scale biological data sets. PLoS One **2:** e718.

Wolinski, H., Kolb, D., Hermann, S., Koning, R.I., and Kohlwein, S.D. (2011). A role for seipin in lipid droplet dynamics and inheritance in yeast. J. Cell Sci. **124:** 3894–3904.

Wright, R. (2000). Transmission electron microscopy of yeast. Microsc. Res. Tech. **51:** 496–510.

Xu, N., Zhang, S.O., Cole, R.A., McKinney, S.A., Guo, F., Haas, J.T., Bobba, S., Farese, R.V., Jr., and Mak, H.Y. (2012). The FATP1-DGAT2 complex facilitates lipid droplet expansion at the ER-lipid droplet interface. J. Cell Biol. **198:** 895–911.

Yang, H., Galea, A., Sytnyk, V., and Crossley, M. (2012). Controlling the size of lipid droplets: lipid and protein factors. Curr. Opin. Cell Biol. **24:** 509–516.

Zehmer, J.K., Huang, Y., Peng, G., Pu, J., Anderson, R.G., and Liu, P. (2009). A role for lipid droplets in inter-membrane lipid traffic. Proteomics **9:** 914–921.

Supplemental Figure 1. Deduced polypeptide sequence alignment of SEIPIN homologues in yeast, human and Arabidopsis. The alignment was generated by Clustal Omega. Asterisks indicate positions which have a single, fully conserved residue. Colons indicate conservation between groups of strongly similar properties. Periods indicate conservation between groups of weakly similar properties. Red: small and mostly hydrophobic residues (A, V, F, P, M, I, L and W). Blue: acidic residues (D and E). Magenta: basic residues (R and K). Green: hydroxyl, sulfhydryl, amine residues and G (S, T, Y, H, C, N, G and Q). Transmembrane domains conserved with human SEIPIN and yeast SEIPIN were predicted by TMHMM and highlighted in grey.

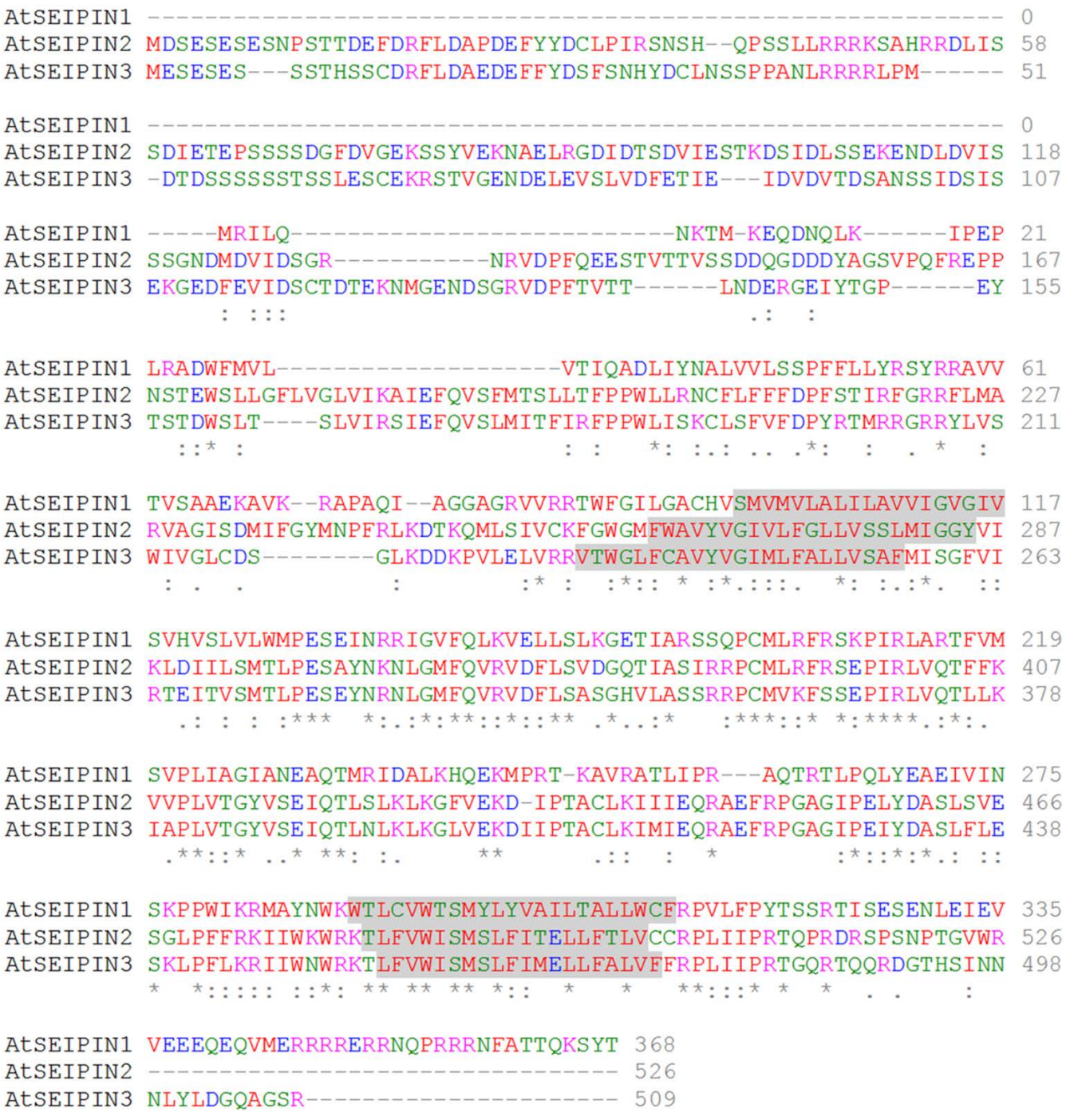

Supplemental Figure 2. Deduced polypeptide sequence alignment of SEIPIN homologues in Arabidopsis. The alignment was generated by Clustal Omega. Asterisks indicate positions which have a single, fully conserved residue. Colons indicate conservation between groups of strongly similar properties. Periods indicate conservation between groups of weakly similar properties. Red: small and mostly hydrophobic residues (A, V, F, P, M, I, L and W). Blue: acidic residues (D and E). Magenta: basic residues (R and K). Green: hydroxyl, sulfhydryl, amine residues and G (S, T, Y, H, C, N, G and Q). Transmembrane domains conserved with human SEIPIN and yeast SEIPIN were predicted by TMHMM and highlighted in grey.

Motif 1 E-value=6.5e^{-9}	
HsSEIPIN	GMFLVTISCYTRGGRIISTSSRSVMLHY
ScSEIPIN	LYCQSKTDHLNLDNLLIDVYRGPGPLLG
AtSEIPIN1	GVFQLKVELLSLKGETIARSSQPCMLRF
AtSEIPIN2	GMFQVRVDFLSVDGQTIASIRRPCMLRF
AtSEIPIN3	GMFQVRVDFLSASGHVLASSRRPCMVKF
Consensus Sequence	GMFQVKVDFLSLDGHTIASSRRPCMLHF
Motif 2 E-value=4.2e^{-15}	
HsSEIPIN	IHAHFTGLRYLLYNFPMTCAFIGVASNFTFLSVIVLFSYMQWVWGGIWPRHRFSLQVNIRK
ScSEIPIN	IHPESGIKFRMNFEQGLRNLMLRKRFLSYIIGISIFHCIICVLFFITGCTAFIFVRKGQEK
AtSEIPIN1	LPQLYEAEIVINSKPPWIKRMAYNWKWTLCVWTSMYLYVAILTALLWCFRPVLFPYTSSRT
AtSEIPIN2	IPELYDASLSVESGLPFFRKIIWKWRKTLFVWISMSLFITELLFTLVCCRPLIIPRTQPRD
AtSEIPIN3	IPEIYDASLFLESKLPFLKRIIWNWRKTLFVWISMSLFIMELLFALVFFRPLIIPRTGQRT
Consensus Sequence	IHEHYDAKLYMNYKLPFIKRMIWNWRKTLFVWISMYHFIMCLLFALVCCRPLIFPRTGQRK
Motif 3 E-value=2.4e^{-6}	
HsSEIPIN	GRARRLLLQFGVLFCTILLLLWVSVFLYGSFYYSYMPTVSHLSPVHFYYRTD
ScSEIPIN	VPLNTFNILNGVQFGTKFFQSIKSIPVGTDLPQTIDNGLSQLIPMRDNMEYK
AtSEIPIN1	VRRTWFGILGACHVSMVMVLALILAVVIGVGIVSLYVEKPVVVRDRLFFDYT
AtSEIPIN2	VCKFGWGMFWAVYVGIVLFGLLVSSLMIGGYVINRIADKPFEVKETLNFDYT
AtSEIPIN3	VRRVTWGLFCAVYVGIMLFALLVSAFMISGFVITYLAHEPLVIKESLNFDYT
Consensus Sequence	VRRNWWGIFWAVHVGTVLFQLLVSAFMIGGFVITYMAHKPHVIKEHLNFDYT

Supplemental Figure 3. Amino acid sequences of various motifs shared between SEIPINs in yeast, humans and Arabidopsis. The *E*-value represents the estimated number of a particular motif that would appear in a similarly sized set of random sequences. Blue: Mostly hydrophobic residues (A, C, F, I, L, V, W and M); Green: Polar, non-charged, non-aliphatic residues (N, Q, S and T); Magenta: Acidic residues (D and E); Red: Positively charged residues (K and R); Purple: H; Orange: G; Black: P; Turquoise: Y.

	Motif 1 E-value=2.3e^{-28}
AtSEIPIN1	LWMPESEINRRIGVFQLKVELLSLKGETIARSSQPCMLRFRSKPIRLARTFVMSVPLIAGIANEAQT
AtSEIPIN2	MTLPESAYNKNLGMFQVRVDFLSVDGQTIASIRRPCMLRFRSEPIRLVQTFFKVVPLVTGYVSEIQT
AtSEIPIN3	MTLPESEYNRNLGMFQVRVDFLSASGHVLASSRRPCMVKFSSEPIRLVQTLLKIAPLVTGYVSEIQT
Consensus Sequence	MTLPESEYNRNLGMFQVRVDFLSADGQTIASSRRPCMLRFRSEPIRLVQTFFKIVPLVTGYVNEIQT
	Motif 2 E-value=2.3e^{-16}
AtSEIPIN1	PQLYEAEIVINSKPPWIKRMAYNWKWTLCVWTSMYLY
AtSEIPIN2	PELYDASLSVESGLPFFRKIIWKWRKTLFVWISMSLF
AtSEIPIN3	PELYDASLSVESGLPFFRKIIWKWRKTLFVWISMSLF
Consensus Sequence	PELYDASLFIESKLPFFKRIIWNWRKTLFVWISMYLF
	Motif 3 E-value=1.3e^{-13}
AtSEIPIN2	KDTKQMLSIVCKFGWGMFWAVYVGIVLFGLLVSSLMIGGYVINRIADKPFEVKETLNFDYTKNSPEAYVPISSCAGVECEGSCKESNEMSKIRG
AtSEIPIN3	KDDKPVLELVRRVTWGLFCAVYVGIMLFALLVSAFMISGFVITYLAHEPLVIKESLNFDYTKSSPEAYVPISSCAGVAFGLSGKESIETGKVKG
Consensus Sequence	KDDKQMLEIVCKFGWGMFWAVYVGIMLFGLLVSAFMIGGYVINYIAHKPFEIKETLNFDYTKNSPEAYVPISSCAGVECGGSCKESNEMGKIKG
	Motif 4 E-value=1.9e^{-5}
AtSEIPIN1	AAEKAVKRAPAQIAGGAG
AtSEIPIN2	ACLKIIIEQRAEFRPGAG
AtSEIPIN3	ACLKIMIEQRAEFRPGAG
Consensus Sequence	ACLKIIIEQRAEFRPGAG
	Motif 5 E-value=3.9e^{-2}
AtSEIPIN2	IEFQVSFMTSLLTFPPWLLRNCFLFFFDPFSTIRFGRRF
AtSEIPIN3	IEFQVSLMITFIRFPPWLISKCLSFVFDPYRTMRRGRRY
Consensus Sequence	IEFQVSFMITFIRFPPWLIRNCFLFFFDPYRTMRFGRRY

Supplemental Figure 4. Amino acid sequences of various motifs shared between the three Arabidopsis SEIPINs. The *E*-value represents the estimated number of a particular motif that would appear in a similarly sized set of random sequences. Blue: Mostly hydrophobic residues (A, C, F, I, L, V, W and M); Green: Polar, non-charged, non-aliphatic residues (N, Q, S and T); Magenta: Acidic residues (D and E); Red: Positively charged residues (K and R); Purple: H; Orange: G; Black: P; Turquoise: Y.

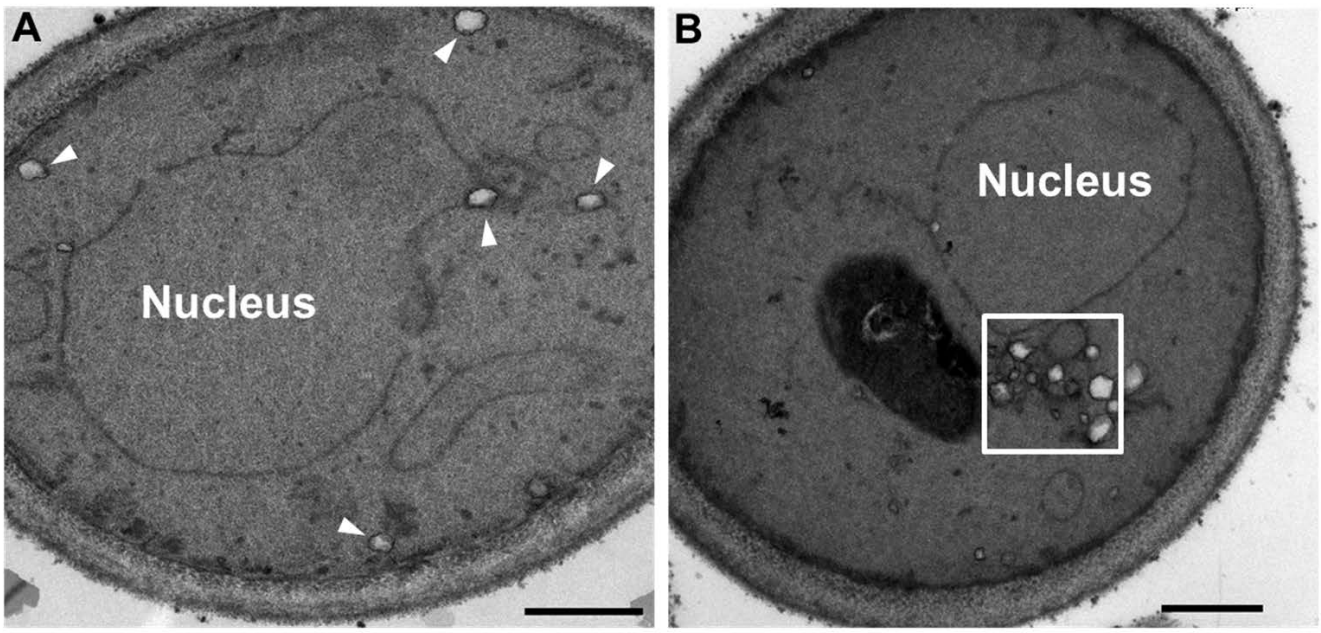

Supplemental Figure 5. Representative electron micrographs of LDs in wild-type yeast, yeast *SEIPIN*-deletion mutant (*ylr404w*Δ), and yeast *SEIPIN*-deletion mutant expressing individual Arabidopsis SEIPINs. The scale bars are 0.5 microns in all panels. (A) LDs (arrowheads) in wild-type yeast. (B) Lipid clusters (white box frame) in yeast *SEIPIN*-deletion mutant (*ylr404w*Δ). (C) Zoom-in image of lipid clusters from boxed region in panel B. (D) Super-sized LD in yeast *SEIPIN*-deletion mutant expressing Arabidopsis SEIPIN1. (E) LDs in yeast *SEIPIN*-deletion mutant expressing Arabidopsis SEIPIN2. (F) LDs in yeast *SEIPIN*-deletion mutant expressing Arabidopsis SEIPIN3.

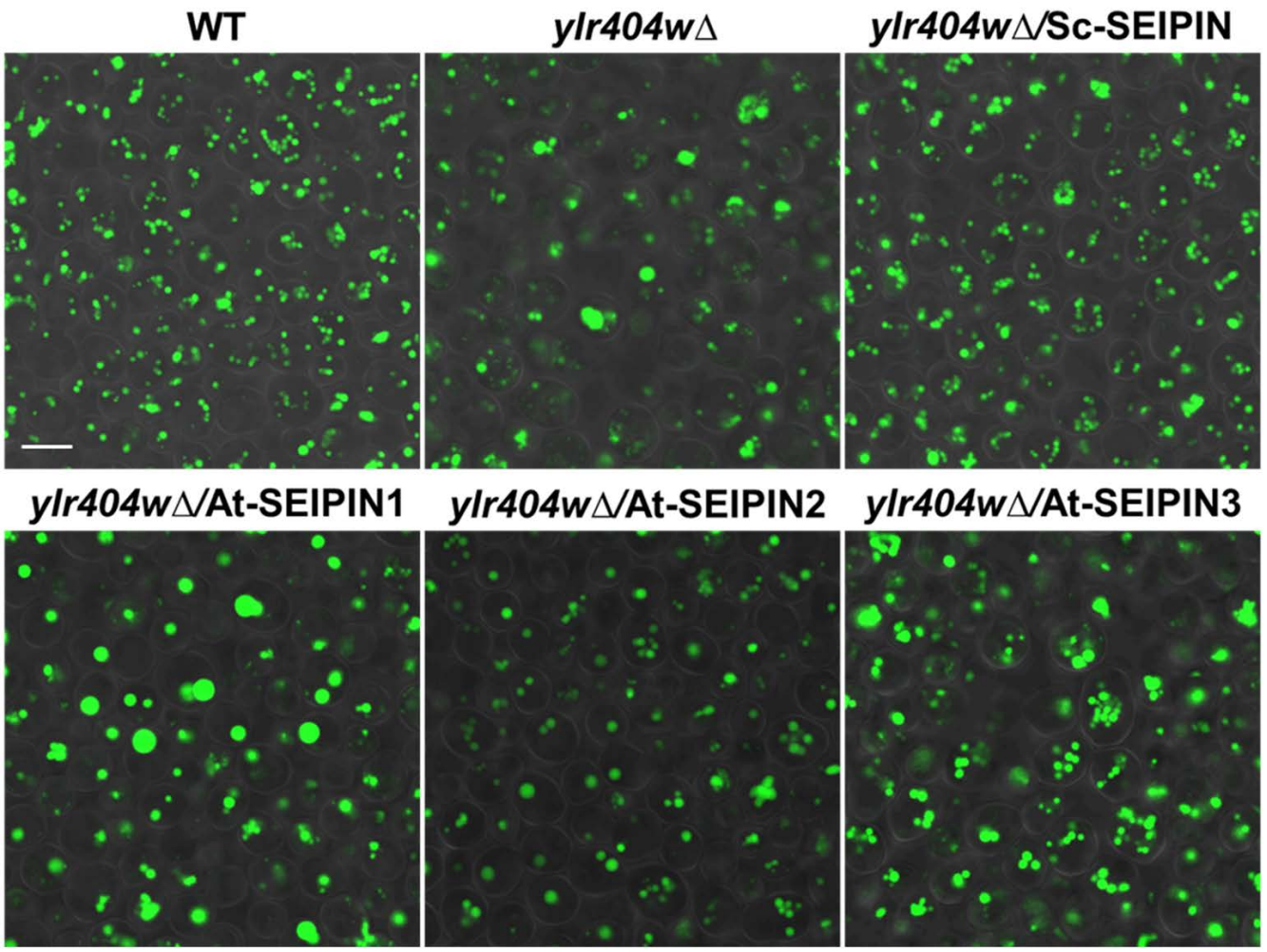

Supplemental Figure 6. Complementation tests for LD phenotypes in the yeast *SEIPIN*-deletion mutant (*ylr404w*Δ, fed with oleic acid) by Arabidopsis SEIPINs compared with functional complementation with yeast SEIPIN. Wild-type (WT) and *ylr404w*Δ were transformed with empty plasmid pRS315. All yeast strains were grown in synthetic complete (SC) medium with oleic acid as the sole carbon source. LDs are stained with BODIPY 493/503 and shown in a false color green. Scale bar = 5 μm.

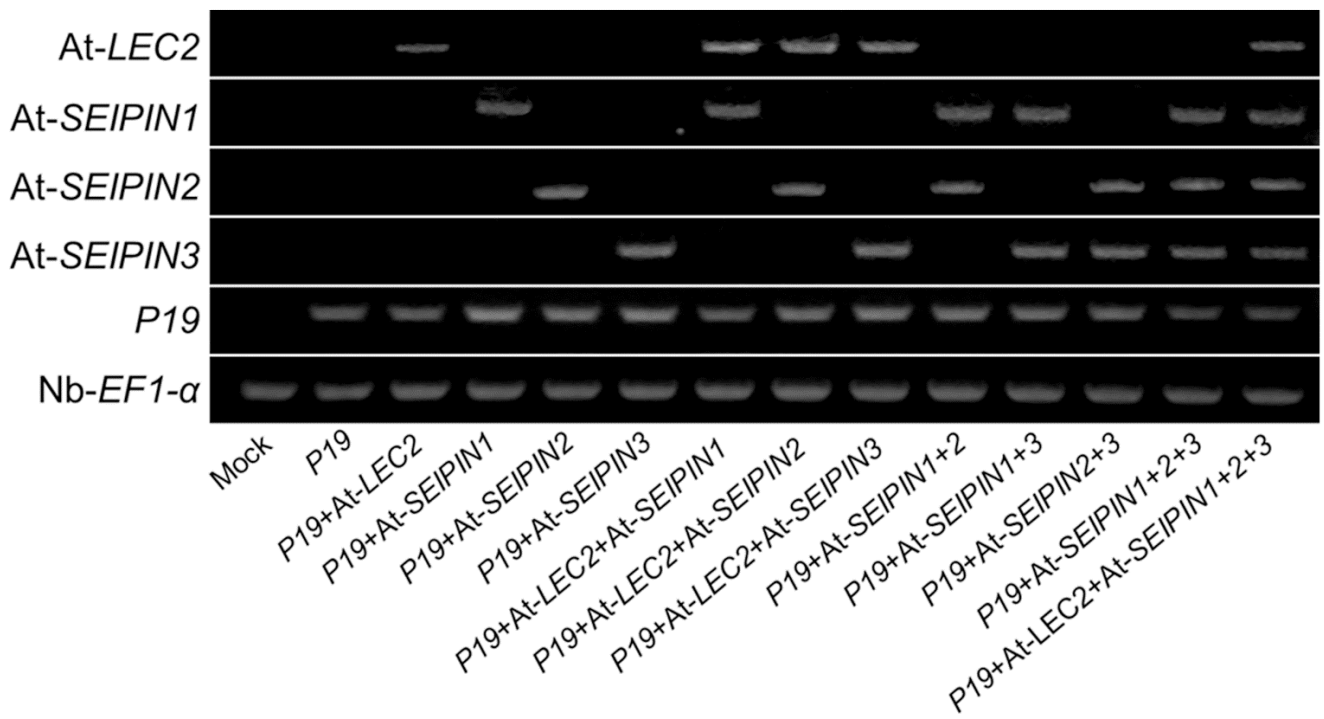

Supplemental Figure 7. Confirmation of the expression of Arabidopsis SEIPINs in tobacco leaves using qualitative RT-PCR. Each lane represents a tobacco leaf sample infiltrated with a mixture of different Agrobacteria carrying the indicated binary plasmids. Mock infection is media only; P19 is used as a viral suppressor of transgene silencing and was included in all treatments.

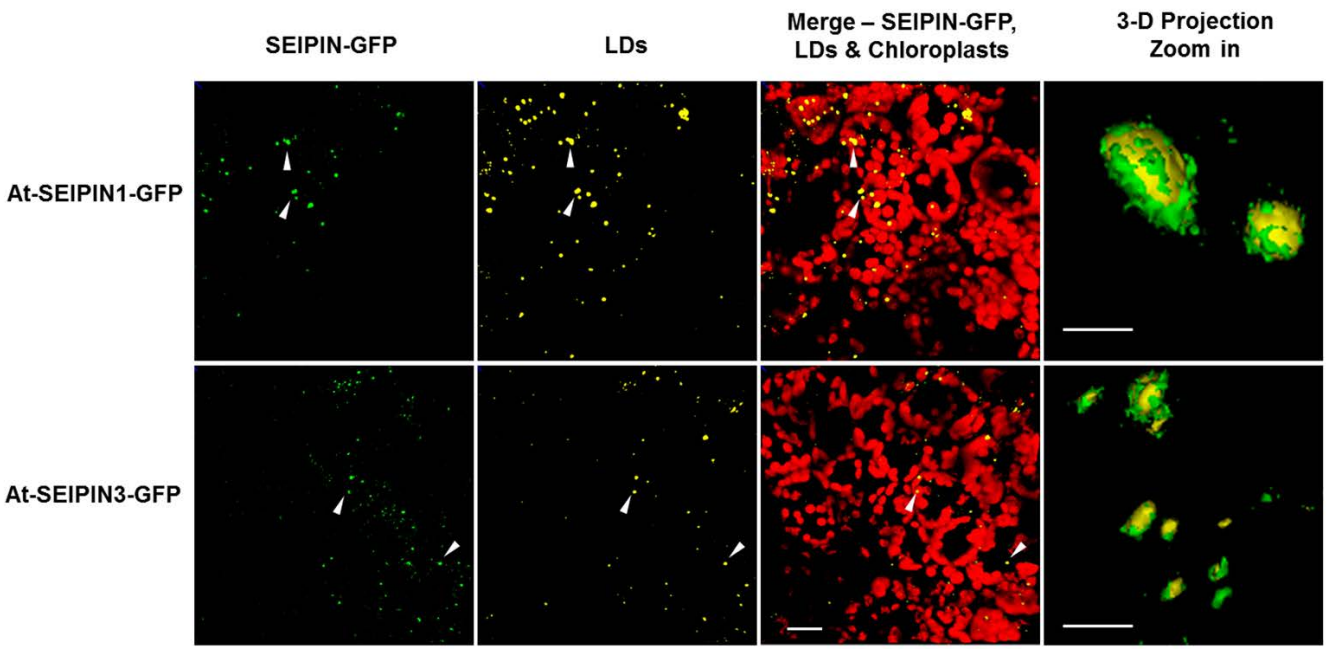

Supplemental Figure 8. Colocalization of LD and Arabidopsis SEIPINs in tobacco leaves. Arabidopsis SEIPINs and LDs are visualized by C-terminal GFP-tagged SEIPIN (green), and Nile Red (yellow), respectively. Red autofluorescence shows chloroplasts. Images were collected at the same magnification and show a 134.82 X 134.82 micron field of the leaf mesophyll. Images are projections of Z-stacks of 27 optical sections taken 0.466 micron apart. P19 is used as a viral suppressor of transgene silencing in all samples. Arrowheads indicate apparent colocalization of LDs and GFP-tagged SEIPINs. Scale bar (first 3 columns) = 20 µm. The last column is 3-D projections of surface rendering Z-stack images showing the colocalization of LDs and GFP-tagged SEIPINs. Scale bars in the last column are all 5 microns.

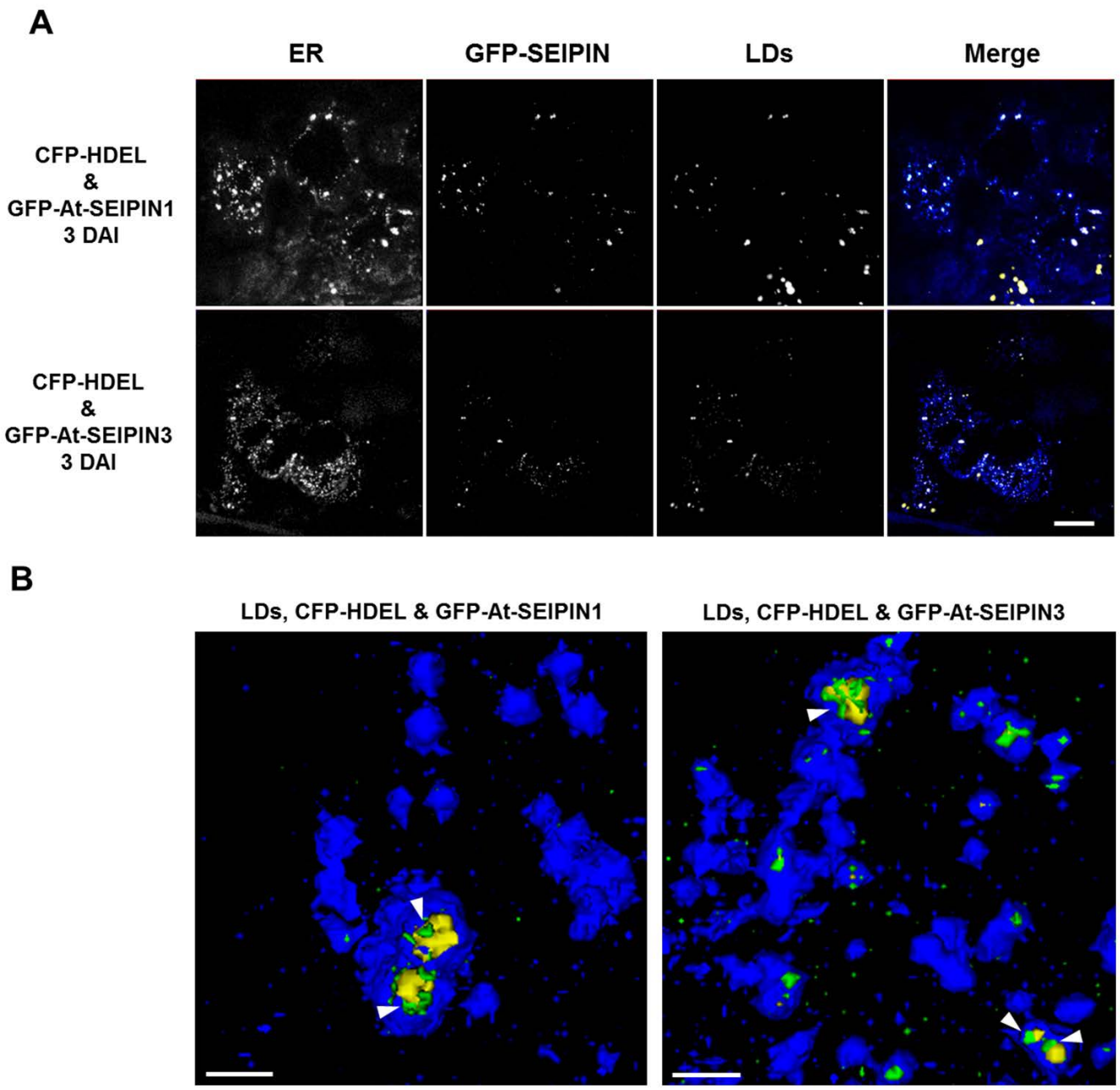

Supplemental Figure 9. Phenotypes of ER organization and LDs at 3 days after infiltration (DAI) of SEIPIN1 or SEIPIN3. (A) Arabidopsis SEIPINs, ER, and LDs were visualized by fluorescence patterns of N-terminal-GFP-tagged SEIPINs, CFP-HDEL, and Nile Red, respectively. All individual channels were shown in grey-scale. GFP, CFP-HDEL, Nile Red, and colocalization were shown in green, blue, yellow, and white respectively in the combined channel. Images are all projections of Z-stacks and the thicknesses of stacks varies from 8 to 12 microns to include all CFP signal, GFP signal and LDs in mesophyll in particular areas. The optical sections were taken 0.466 micron apart. P19 was used as a viral suppressor of transgene silencing in all samples. Scale bar = 20 μm. (B) Three-dimensional projections of surface rendering Z-stack images showing the colocalization of LDs, ER and GFP-tagged SEIPINs. The scale bars are all 5 microns in panel B. Arrowheads indicate localizations of GFP-tagged SEIPIN.

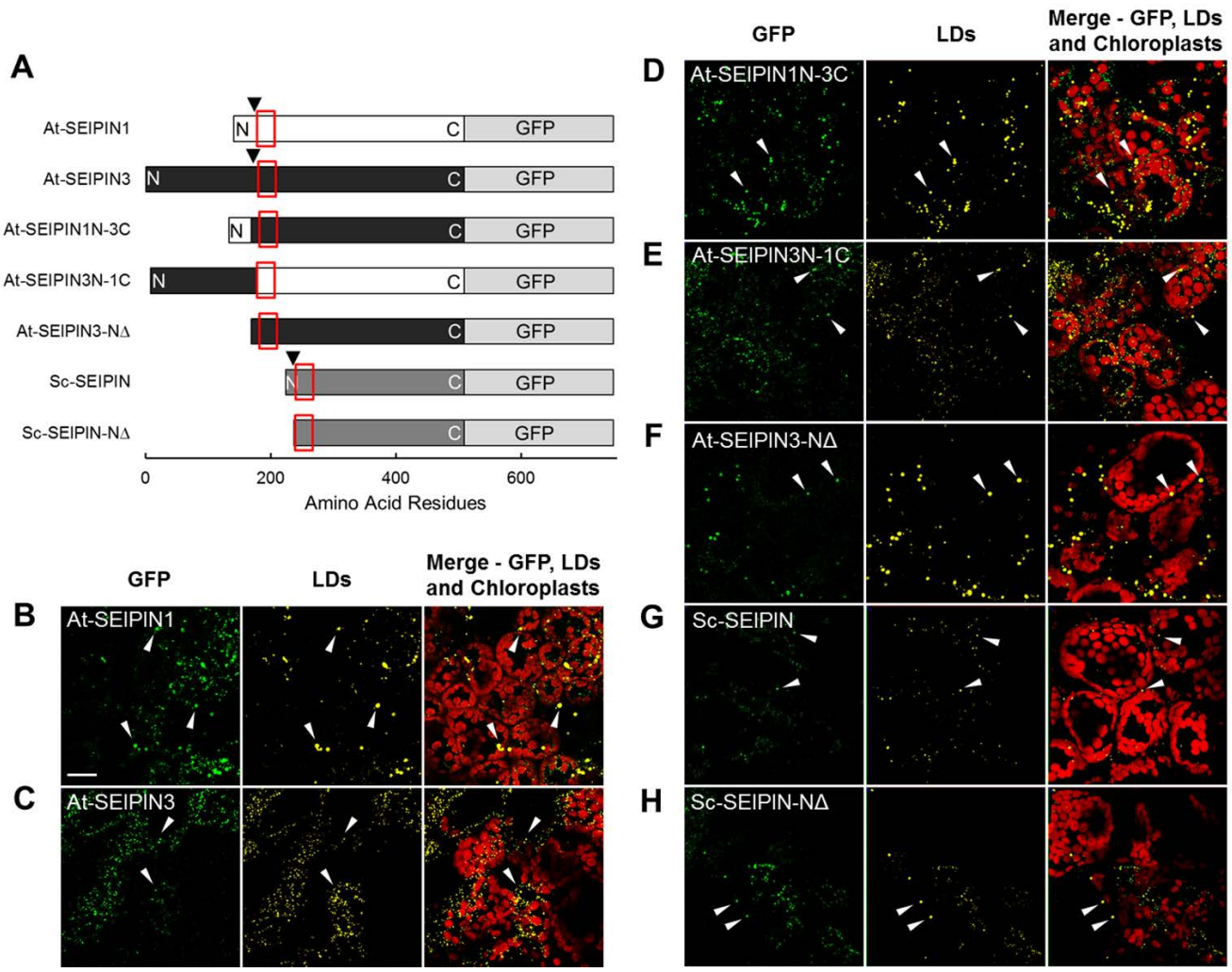

Supplemental Figure 10. Localization of domain-swapped/truncated Arabidopsis and yeast SEIPINs in tobacco leaves. (A) Diagram of domain swaps and truncations in At-SEIPIN1, At-SEIPIN3 and Sc-SEIPIN. Black arrowheads indicate the cutting sites on wild-type At-SEIPIN1, At-SEIPIN3 and Sc-SEIPIN. Red box frames indicate the first predicted transmembrane domains in At-SEIPIN1, At-SEIPIN3 and Sc-SEIPIN. (B, C, D, E, F, G, and H) Colocalization of LDs and domain-swapped/truncated Arabidopsis and yeast SEIPINs in tobacco leaves. SEIPINs and LDs are visualized by C-terminal GFP-appended SEIPIN (green), and Nile Red (yellow), respectively. Red autofluorescence shows chloroplasts. Images were collected as described in Supplemental Figure 8. P19 is used as a viral suppressor of transgene silencing in all samples. Arrowheads indicate apparent colocalization of LDs and GFP-tagged SEIPINs. Scale bar (shown in panel B) = 20 μm. Images were collected at same magnification and show a 134.82 X 134.82 micron field of the leaf mesophyll. (B) Wild-type At-SEIPIN1. (C) Wild-type At-SEIPIN3. (D) Domain-swapped At-SEIPIN1N-3C. (E) Domain-swapped At-SEIPIN3N-1C. (F) Domain-truncated At-SEIPIN3-NΔ. (G) Wild-type Sc-SEIPIN. (H) Domain-truncated Sc-SEIPIN-NΔ.

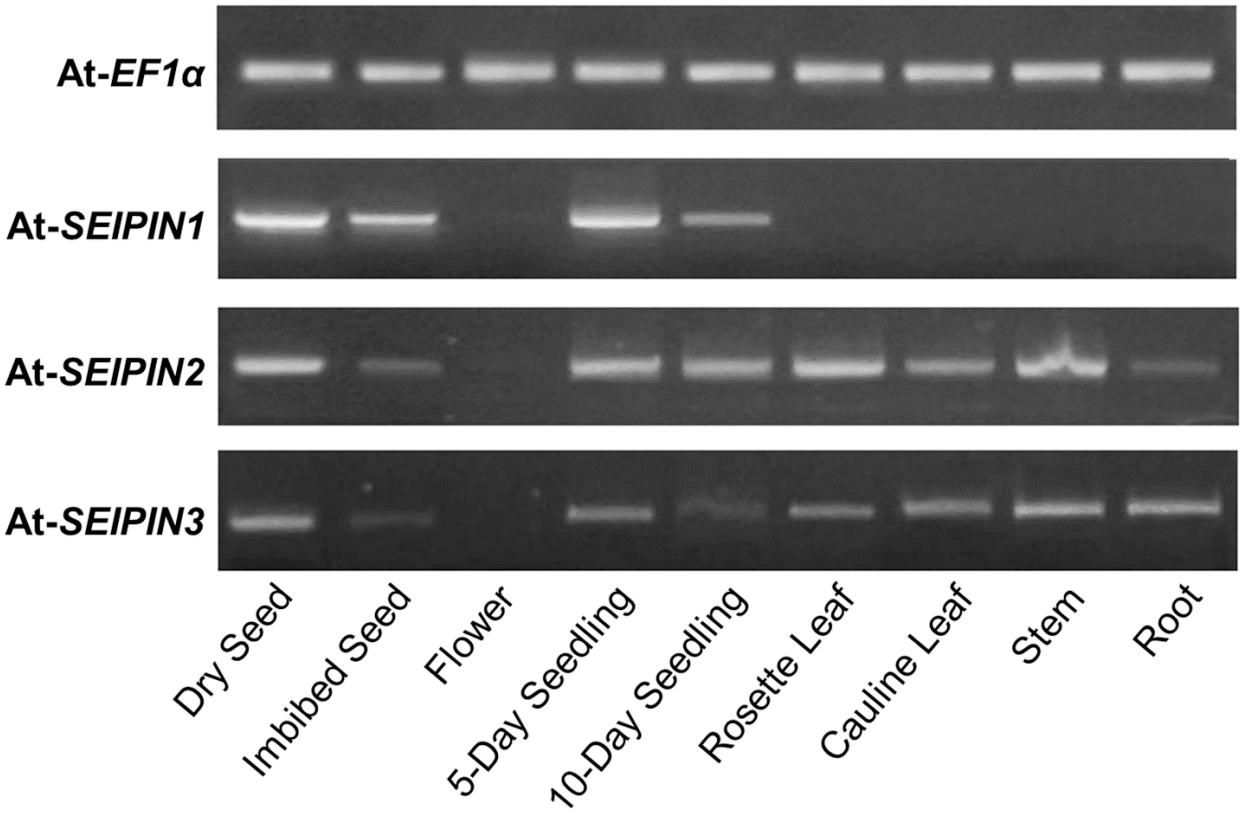

Supplemental Figure 11. Analysis of expression patterns of Arabidopsis SEIPINs in different tissues and developmental stages by using RT-PCR. Arabidopsis elongation factor 1-alpha gene (*EF1α*) is included as reference gene. Rosette leaf and root tissues are sampled from four-week-old plants. Cauline leaf, stem and flower tissues are collected from six-week-old plants. Imbibed seeds are placed on wet filter paper and incubated in the Arabidopsis growth chamber for 24 hours.

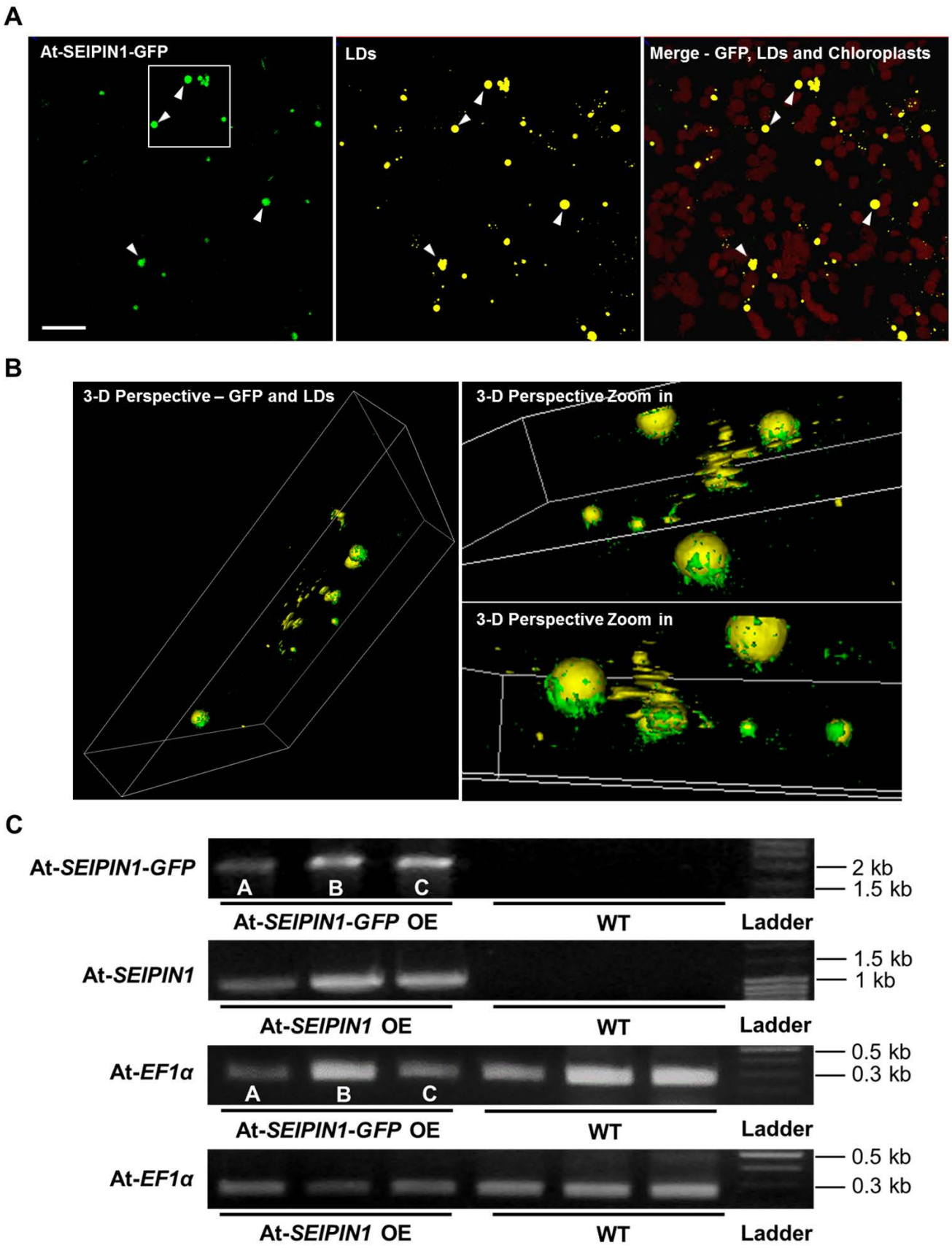

Supplemental Figure 12. Expression and localization of SEIPIN1 in Arabidopsis leaves. (A) Colocalization of GFP-tagged SEIPIN1 and LDs (Nile Red, yellow). Red color shows chloroplast autofluorescence. Images were collected at the same magnification and show a 134.82 X 134.82 micron field of the leaf mesophyll. Images are projections of Z-stacks of 30 optical sections taken 0.466 micron apart. Arrowheads indicate apparent colocalization of LDs and GFP-tagged SEIPIN1. White box indicates the region shown in higher magnification in panel B. Scale bar = 20 µm. (B) Three-dimensional perspectives of surface rendering, high magnified (zoom in) Z-stack images of selected regions in panel A (white box frame) showing the colocalization of LDs and GFP-tagged SEIPINs. Supplemental Movie 6 is associated with the 3-D perspectives in panel B. (C) Confirmation of the expression of SEIPIN1 in Arabidopsis leaves using RT-qPCR. *EF1α* was used as a reference gene. SEIPIN1-GFP OE-A, B, and C are three independent transgenic events.

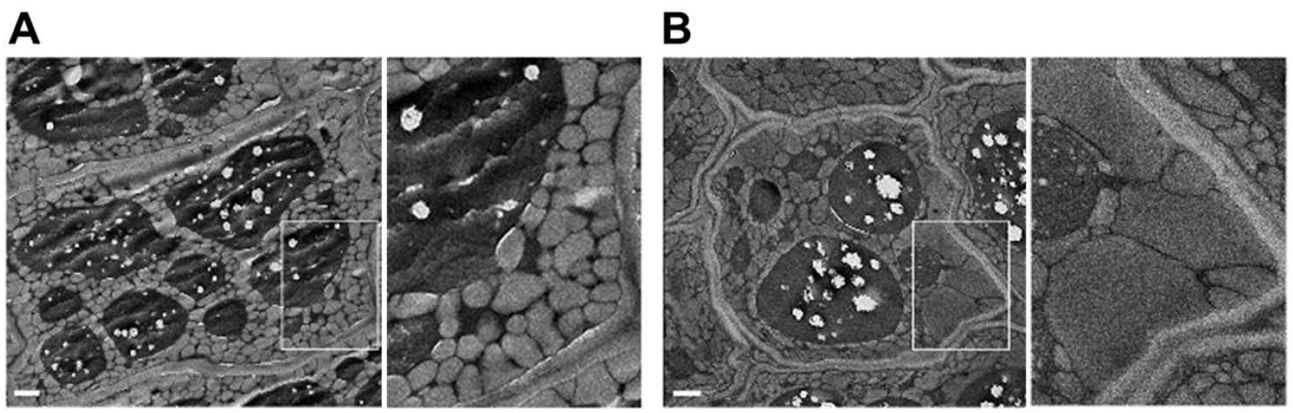

Supplemental Figure 13. Representative electron micrographs of LDs in wild-type and SEIPIN1 over-expressing Arabidopsis seeds. The scale bars are 1 micron. (A) LDs in cotyledonary cells of a wild-type, mature seed embryo. (B) Large-sized LDs in cotyledon cells of an SEIPIN1 mature seed embryo. White boxes in (A) and (B) represent portions of the cell shown at higher magnification in the panels to the right; note the relatively large-sized LDs in (B).

Supplemental Table 1. Names and sequences of primers used in this study.

Primer Name	Sequence
S1FP1	5′- GGCGCGCCAATGAGAATCCTCCAAAAC -3′
S1RP1	5′- TTAATTAACTATGTATAACTTTTCTGTGTAG -3′
S2FP1	5′- GGCGCGCCAATGGACTCCGAGTCCGAGT -3′
S2RP1	5′- TTAATTAACTACCTCCAGACTCCAGT -3′
S3FP1	5′- GGCGCGCCAATGGAATCAGAATCAGAATCATCA -3′
S3RP1	5′- TTAATTAATCATCTACTTCCCGCCTGA -3′
S1NFP	5′- GGGCCCTTAATTAAATGAGAATCCTCCAAAACAAAAC -3′
S1NARP	5′- CATCAAACTAACTTGAAATTCAATATCAGCTTGGATGGTGAC -3′
S3CAFP	5′- GTCACCATCCAAGCTGATATTGAATTTCAAGTTAGTTTGATG -3′
S3CRP	5′- GGGCCCGGCGCGCCATCTACTTCCCGCCTGAC -3′
S3NFP	5′- GGGCCCTTAATTAAATGGAATCAGAATCAGAATCATC -3′
S3NARP	5′- CACGAGTGCGTTGTAGATTAGTGACCTGATCACTAGACTCG -3′
S1CAFP	5′- CGAGTCTAGTGATCAGGTCACTAATCTACAACGCACTCGTG -3′
S1CRP	5′- GGGCCCGGCGCGCCATGTATAACTTTTCTGTGTAGTAGC -3′
S3TAFP	5′- GGGCCCTTAATTAAATGATTGAATTTCAAGTTAGTTTGATGATTAC -3′
SYFP	5′- GGGCCCTTAATTAAATGAAAATCAATGTATCCCGTCC -3′
SYRP	5′- GGGCCCGGCGCGCCAGCTATGTTTCTTGGATTTTTCCTG -3′
SYTFP	5′- GGGCCCTTAATTAAATGAGTTCATATATTGTTGTTGCATTTC -3′
S1D-miR1	5′- GATGTAACATACAAGGTCGGCTCTCTCTCTTTTGTATTCC -3′
S1D-miR2	5′- GAGAGCCGACCTTGTATGTTACATCAAAGAGAATCAATGA -3′
S1D-miR3	5′- GAGAACCGACCTTGTTTGTTACTTCACAGGTCGTGATATG -3′
S1D-miR4	5′- GAAGTAACAAACAAGGTCGGTTCTCTACATATATATTCCT -3′
Oligo-miR-A	5′- GGCGCGCCCTGCAAGGCGATTAAGTTGGGTAAC -3′
Oligo-miR-B	5′- TTAATTAAGCGGATAACAATTTCACACAGGAAACAG -3′
GFPRP	5′- TTAGTGGTGGTGGTGGTGGTGT -3′
S1FP2	5′- ATGAGAATCCTCCAAAACAAAAC -3′
S1RP2	5′- TAACTTTTCTGTGTAGTAGCAAAATTTCTT -3′
S2FP2	5′- ATGGACTCCGAGTCCGAG -3′
S2RP2	5′- CTACCTCCAGACTCCAGT -3′
S3FP2	5′- ATGGAATCAGAATCAGAATCATCA -3′
S3RP2	5′- TCATCTACTTCCCGCCTGA -3′
LEC2FP	5′- CGCTCGCACTTCACAACAGTCCC -3′
LEC2RP	5′- CATCGGATGAACCCACGTACGCG -3′
P19FP	5′- ATGGAACGAGCTATACAAGGAAACG -3′
P19RP	5′- CAGGGCATCCTCTTGATTCATTAC -3′
EFFP	5′- ACTGCACTGTGATTGATGCC -3′
EFRP	5′- GACACCAGTTTCCACACGAC -3′
EF1αFP	5′- AGGTCCACCAACCTTGACTG -3′
EF1α RP	5′- GAGACTCGTGGTGCATCTCA -3′
S1qFP	5′- GAGATCGTTTAGTGTTCCTGTTGGTCATAGTGTTC -3′
S1qRP	5′- GTAACATACAAGGTTGGCTCGATCTCGCG -3′